

Revised stratigraphy and geochronology of the Hazelton Group, host rocks for volcanogenic mineralization in the Kitsault River area, northwestern British Columbia



Rebecca C. Hunter^{1, a}, Christopher F.B. Sebert², Richard Friedman³, and Corey Wall³

¹ British Columbia Geological Survey, Ministry of Energy, Mines and Low Carbon Innovation, Victoria, BC, V8W 9N3

² Dolly Varden Silver Corporation, Vancouver, BC, V7X 1E5

³ Pacific Centre for Isotopic and Geochemical Research, Department of Earth, Ocean and Atmospheric Sciences, The University of British Columbia, Vancouver, BC, V6T 1Z4

^a corresponding author: Rebecca.Hunter@gov.bc.ca

Recommended citation: Hunter, R.C., Sebert, C.F.B., Friedman, R., and Wall, C., 2022. Revised stratigraphy and geochronology of the Hazelton Group, host rocks for volcanogenic mineralization in the Kitsault River area, northwest British Columbia. In: Geological Fieldwork 2021, British Columbia Ministry of Energy, Mines and Low Carbon Innovation, British Columbia Geological Survey Paper 2022-01, pp. 63-81.

Abstract

The Kitsault River area, at the southern end of the ‘Golden Triangle’, hosts numerous Ag-rich volcanogenic massive sulphide (VMS) and epithermal-type deposits similar to those of the Eskay rift ca. 150 km to the northwest. Resolving the age and affinity of late Early to Middle Jurassic volcano-sedimentary Hazelton Group host rocks is key to understanding the metallogeny of the Kitsault River area. Based on field and new U-Pb zircon geochronological data we identify six Hazelton Group facies in the Kitsault area. The lower Hazelton Group consists of facies 1, a coarse-grained basal unit of sedimentary rocks with a maximum depositional age of ca. 206-204 Ma; facies 2, a volcano-sedimentary package with abundant limestone, tuff and lapilli tuff to tuff breccia with augite-phyric clasts and a crystallization age of ca. 201 Ma; facies 3, an andesitic lapilli tuff to tuff breccia package with abundant exotic clasts (chert, limestone) and epiclastic beds, and facies 4, an andesitic lapilli tuff to tuff breccia unit with volcanic-derived clasts and rare sedimentary beds with a crystallization age of ca. 193 Ma. Upper Hazelton Group strata consist of facies 5, a unit of fine grained tuffaceous and epiclastic rocks of rhyodacite to basalt composition with a maximum depositional age of 188 to 178 Ma and facies 6, a unit of interbedded feldspathic wacke and tuff with a maximum depositional age of ca. 168 Ma. The VMS and VMS-related epithermal occurrences in the Kitsault River area are in rocks of the upper Hazelton Group. The new maximum depositional age (ca. 188 Ma) of epiclastic rocks from the Sault Zn-Pb-Ag-Sr showing suggests that the VMS mineralization in the Kitsault River area may be slightly older than the ca. 174 Ma Au-rich VMS systems of the Eskay rift and indicates that significant precious metal-bearing VMS and/or epithermal-type systems formed well outside the main Eskay rift corridor in mainly volcanoclastic rocks.

Keywords: Kitsault River, Hazelton Group, Stikinia, Jurassic, U-Pb zircon geochronology, VMS, Eskay rift, Golden Triangle, silver, gold

1. Introduction

Deciphering the stratigraphic and timing relationships of rocks deposited in volcano-sedimentary regions is challenging because of abrupt vertical and lateral variability, high rate of deposition and erosion, and disruption by synvolcanic structures (e.g., Gibson et al., 1999; Marti et al., 2018). To establish such relationships in regions of prolonged volcanic activity, detailed mapping and facies analysis supplemented by abundant geochronological sampling are needed.

The Kitsault River area is ca. 50 km southeast of Stewart along the west-central margin of Stikinia (Fig. 1) and at the southern end of the Iskut-Stewart mineral belt, which forms part of the informally named ‘Golden Triangle’ (Fig. 2). It is within the traditional lands of the Nisga’a, Gitanyow, Tsetsaut Skii Km Lax Ha, and Metlakatla First Nations. The area hosts significant Ag-rich volcanogenic massive sulphide (VMS) deposits and showings (e.g., Dolly Varden, Torbrit, Wolf, Sault) in late Early to Middle Jurassic volcano-sedimentary rocks of the upper Hazelton Group. The host rocks were originally

included in a lower Hazelton Group intermediate volcanic unit (IJHvc Fig. 3; Alldrick et al., 1986). A ca. 193 Ma U-Pb zircon age on a dacite in the footwall of the Sault showing (Mortensen and Kirkham, 1992) is consistent with ages in the lower Hazelton Group (Johnny Mountain dacite; Nelson et al., 2018). However, an upper Hazelton rhyolitic lapilli tuff from the Wolf deposit area yielded a preliminary CA-TIMS crystallization age of ca. 178 Ma (Hunter and van Straaten, 2020). This significantly younger age suggests that some or all the host rocks may be part of the upper Hazelton Group, coeval with the Iskut River Formation in the Eskay rift (Gagnon et al., 2012). Resolving the age and affinity of the host rocks is key to understanding the metallogeny of the Kitsault River area.

In this paper we refined the stratigraphy of the Hazelton Group based on mapping in the Kitsault River area and present three new CA-TIMS and three LA-ICPMS U-Pb zircon ages. These additional data help to decipher the timing of volcanism and sedimentation that were ultimately responsible for VMS- and/or epithermal mineralizing systems in the Kitsault River

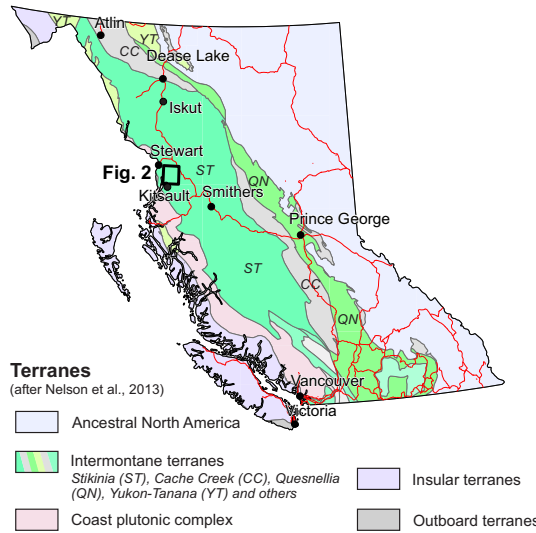


Fig. 1. Simplified terrane map of British Columbia (after Nelson et al., 2013) and location of Kitsault study area.

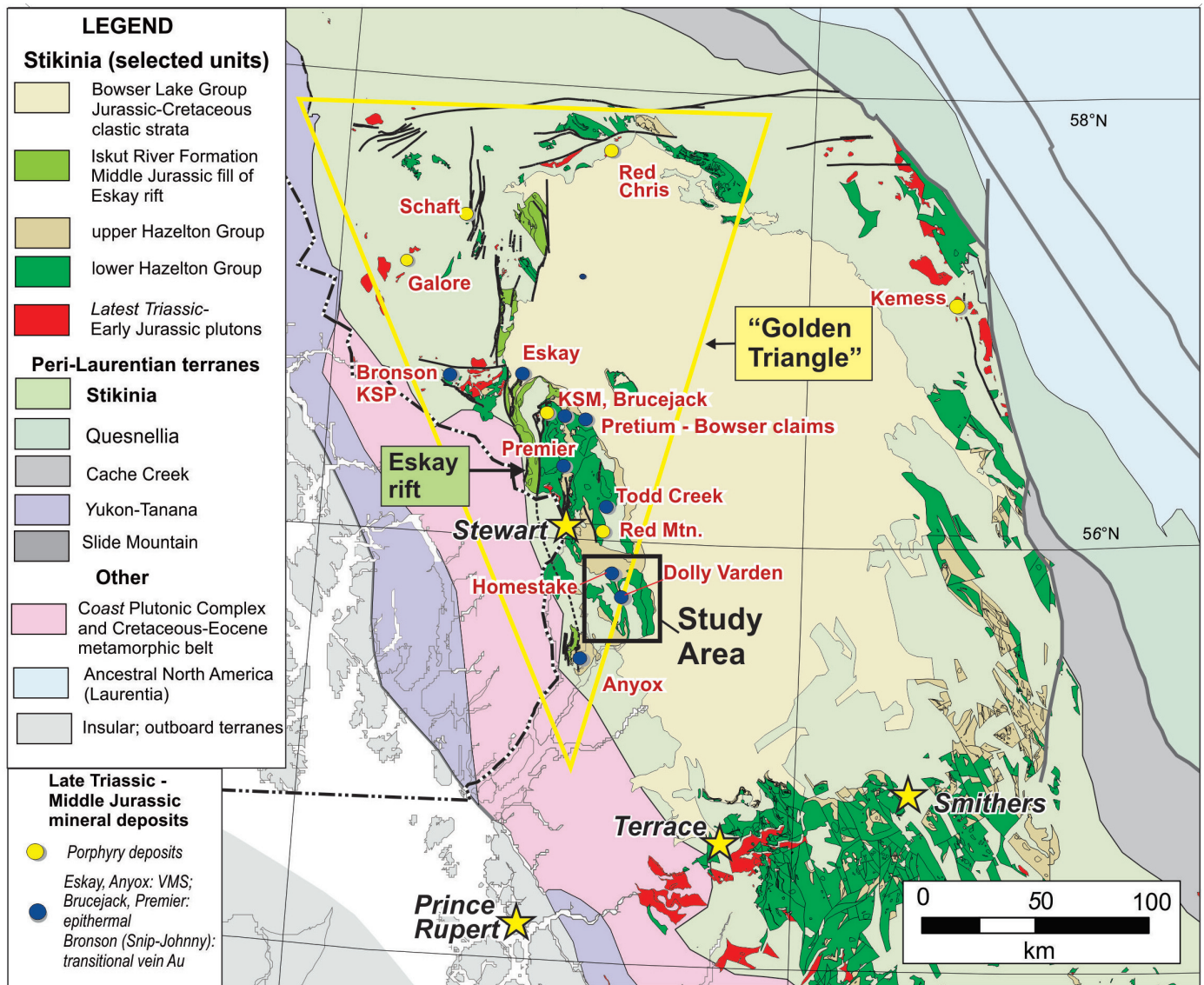
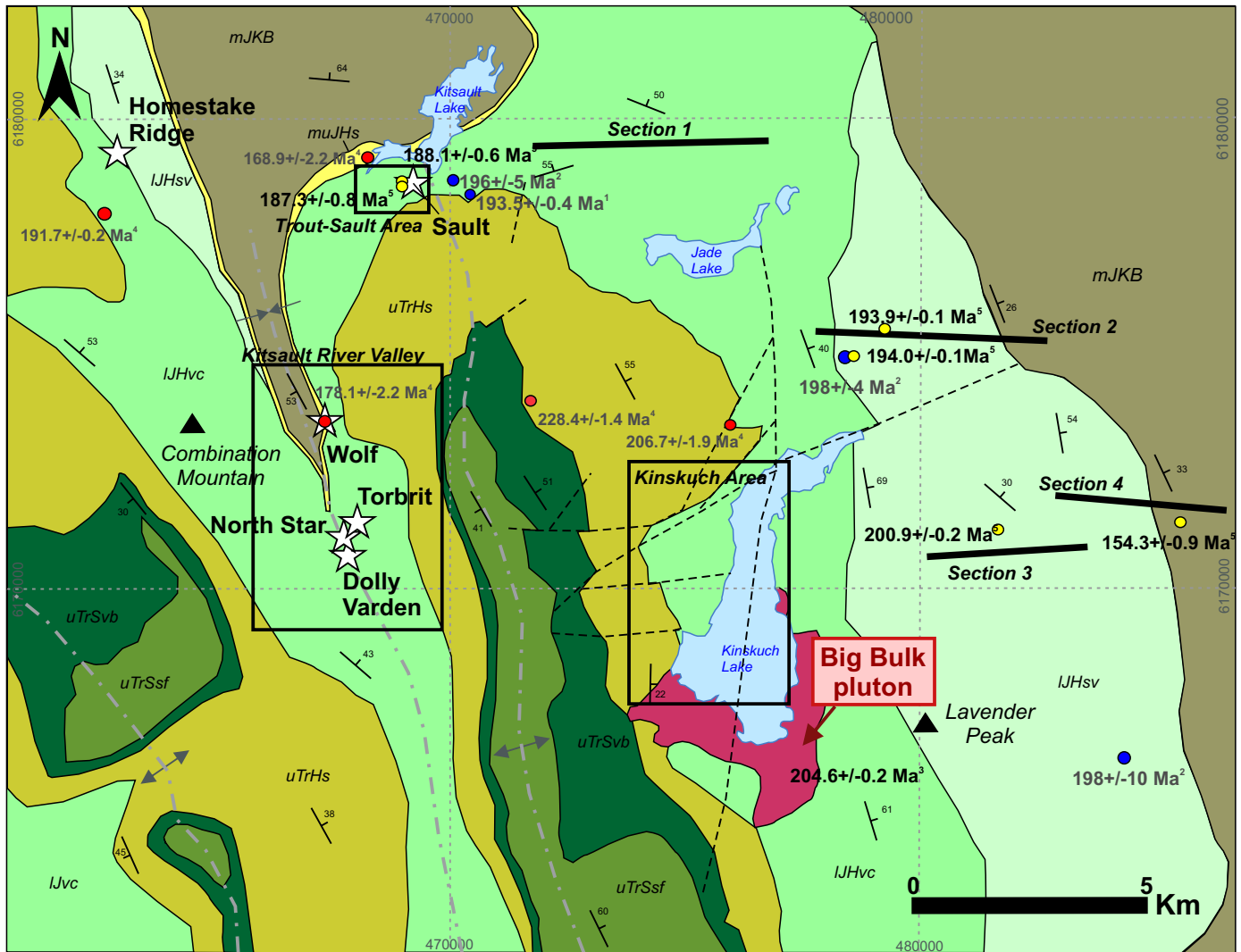


Fig. 2. Kitsault River study area with respect to major Late Triassic to Middle Jurassic mineral deposits in northwestern Stikinia (after Nelson et al., 2018).



Legend

Bowser Lake Group (Middle Jurassic)

mJKB mudstone, sandstone, chert pebble conglomerate

Hazelton Group (Lower-Middle Jurassic)

muJHs upper sedimentary unit - Quock Fm.

IJHsv epiclastic and felsic volcanic unit

IJHvc intermediate volcanic unit

uTrHs middle sedimentary unit (transitional)

Stuhini Group (Upper Triassic)

uTrSvb mafic volcanic unit

uTrSsf lower sedimentary unit

- This study
- Hunter and van Straaten, 2020
- Historical ages
- ☆ Deposits
- - - Faults
- Axial trace
- Bedding

Fig. 3. Simplified geology of the Kitsault River area (after Alldrick et al., 1986; MacIntyre et al., 1994). Sources of geochronology: ¹Mortensen and Kirkham, 1992; ²Greig and Gehrels, 1995; ³Miller et al., 2020; ⁴Hunter and van Straaten, 2020; ⁵this study. Stratigraphic subdivisions are those of Alldrick et al., 1986 (cf. Table 1, Fig. 4).

area. Although the Kitsault River area lies approximately 30 km east of the projected extent of the Eskay rift, new data suggest that VMS and VMS feeder mineralization may be both Eskay rift equivalent and older.

2. Regional geology

Stikinia, a polyphase island arc terrane, is made up of the Stikine assemblage (Devonian to Mississippian; Anderson, 1989; Greig, 1992; Logan et al., 2000), the Stuhini and Takla groups (Middle to Late Triassic; Monger, 1977; Brown et al., 1996), and the Hazelton Group (latest Triassic to Middle Jurassic; Marsden and Thorkelson, 1992; Gagnon et al., 2012; Nelson et al., 2018).

The Stuhini Group consists of augite-rich basalt to basaltic andesite, crystal-lithic lapilli tuff, and epiclastic strata including greywacke, siltstone, tuff, and limestone (Brown et al., 1996). The Hazelton Group overlies the Stuhini Group and older rocks along a regional unconformity (Greig, 2014; Nelson and Kyba, 2014) and is an extensive package of volcanic and sedimentary rocks (Marsden and Thorkelson, 1992; Gagnon et al., 2012; Nelson et al., 2018). Regionally, the lower Hazelton Group comprises siliciclastic rocks of the Jack Formation (cobble to boulder granitoid-clast conglomerate, granulestone, arkosic sandstone, and thinly bedded siltstone and mudstone), the Snippaker unit (sandstone, polymictic conglomerate, siltstone and mudstone), and the Klastline and Betty Creek formations, including the Unuk River andesite unit (andesitic and lesser felsic volcanoclastic rocks; Gagnon et al., 2012; Nelson et al., 2018 and references therein). The upper Hazelton Group consists of sedimentary rocks of the Spatsizi Formation (volcanic-derived sandstone, conglomerate, mudstone, siltstone and limestone) and Quock Formation (siliceous mudstone and pale felsic tuff), subaerial dacite and rhyolite flows of the Mount Dilworth Formation, and bimodal volcanic and sedimentary rocks of the Iskut River Formation (Gagnon et al., 2012; Nelson et al., 2018). The Bowser Lake Group (Middle Jurassic to Middle Cretaceous) overlies the Hazelton Group and consists of marine and nonmarine sandstones, siltstones, and conglomerates (Tipper and Richards, 1976; Eisbacher, 1981; Evenchick and Thorkelson, 2005; Evenchick et al., 2007).

The study area hosts porphyry (e.g., Big Bulk), precious and base metal-rich epithermal (e.g., Homestake Ridge), and VMS (e.g., Dolly Varden, Torbrit, Wolf) deposits and showings, which formed in volcano-sedimentary successions of the Hazelton Group and associated plutonic rocks of Stikinia (Fig. 2; Höy, 1991; Childe, 1997; Nelson et al., 2013; Logan and Mihalyuk, 2014; Barresi et al., 2015; Nelson et al., 2018). The Big Bulk porphyry Cu showing, spatially and temporally related to the sub-Hazelton unconformity, formed during the Rhaetian (Miller et al., 2020; Hunter and van Straaten, 2020). Major porphyry deposits (Cu-Au-Ag-Mo) of the Stewart-Iskut district such as the KSM (Kerr-Sulphurets-Mitchell), Brucejack, Silbak-Premier, Big Missouri, Scottie Gold, and Red Mountain deposits, similarly formed during the Latest Triassic to Early Jurassic (Nelson and Kyba, 2014). The Homestake

Ridge epithermal deposit possibly formed in the Early Jurassic (Hunter and van Straaten, 2020) which, if true, would make it synchronous with deposition of the Betty Creek Formation. Most of the major VMS deposits (e.g., Eskay Creek, Anyox) of the Stewart-Iskut district are in upper Hazelton Group rocks (Lower to Middle Jurassic) of the Iskut River Formation in the Eskay rift (Barresi et al., 2015). However, several VMS deposits and showings are in mixed sedimentary to intermediate to felsic pyroclastic rocks 10s of kilometres outside the Eskay rift (e.g., Dolly Varden, Wolf, Torbrit, Todd Creek, Pretium-Bowser project showings, Premier-Silver Hill; Hunter and van Straaten, 2020).

3. Geology of the Kitsault area

In the Kitsault area, Triassic to Cretaceous volcano-sedimentary rocks of the Stuhini, Hazelton and Bowser Lake groups form continuous, tightly folded, north-northwest-trending anticline-syncline pairs (Fig. 3; Alldrick et al., 1986; Dawson and Alldrick, 1986; Greig, 1991; Evenchick et al., 2008). Alldrick et al. (1986) loosely subdivided the area into two broad Stuhini Group volcano-sedimentary units, a middle sedimentary unit, and two Hazelton Group units, including an intermediate volcanic rock unit and an epiclastic and felsic volcanic unit that grades upward into sedimentary strata of the Bowser Lake Group (Fig. 3; Table 1).

The Stuhini Group, the oldest unit in the area consists of black siltstone, mudstone, feldspathic wacke, conglomerate, basalt, pyroclastic rock and local limestone. Alldrick et al. (1986) and Devlin (1987) separated the Stuhini Group into a 'lower sedimentary unit' and a 'mafic volcanic unit' (units uTrSsf and uTrSvb, Fig. 3).

The lowest part of the Hazelton Group section as mapped by Alldrick et al. (1986) is a basal unit consisting of siltstone, sandstone, wacke, conglomerate, and volcanic breccia containing limestone clasts (unit uTrHs, Fig. 3). Detrital zircons from basal Hazelton Group volcanic-derived sandstone and polymictic pebble conglomerate yielded preliminary maximum depositional ages of 228.4 ± 1.4 Ma and 206.7 ± 1.9 Ma (Hunter and van Straaten, 2020). Recent work in the Kinskuch Lake area showed that this basal unit is more extensive than mapped by Alldrick et al. (1986) and includes impressive megaclast-bearing conglomerate (with clasts up to 120 m) that formed along prominent northeast-trending faults (Kinskuch conglomerates; Miller et al., 2020). These faults were active as early as the latest Triassic and display strike-slip to oblique slip movement, interpreted to have resulted in local zones of extension and small, pull-apart basins (Miller et al., 2020). The emplacement of the Big Bulk porphyry stock (Fig. 3; 204.61 ± 0.18 Ma) and associated Cu-Au mineralization is interpreted to coincide this period of extension (Miller et al., 2020). Late Triassic normal faulting and deposition of coarse conglomerates during the transition from the Stuhini Group to the Hazelton Group is reported throughout the Stewart-Iskut district (Nelson and Kyba, 2014; Kyba and Nelson, 2015; Febbo et al., 2019).

Table 1. Evolution of lithostratigraphic subdivisions in the Kitsault area, including informal units used in this study.

		Alldrick et al., 1986	Hunter and van Straaten (2020)	This study
Bowser Lake Group		Bowser Lake Group (mJKB)	Bowser Lake Group	Bowser Lake Group
upper Hazelton Group	Quock Formation	upper sedimentary unit (muJHS)		facies 6
	Spatsizi Formation			facies 5 (Kitsault unit)
lower Hazelton Group	Betty Creek Formation; includes Unuk River andesite unit	epiclastic and felsic volcanic unit (IJHsv) intermediate volcanic unit (IJHvc)	facies 3, sub-facies 3a; facies 1 and 2	facies 3 and 4 sub-facies 4a
		middle sedimentary unit (uTrHs) (transitional)	sub-facies 3b	facies 1 and 2 (Kinskuch unit)
Stuhini Group		mafic volcanic unit (uTrSvb)		
		lower sedimentary unit (uTrSsf)		

The basal Hazelton Group unit is overlain by a thick section of andesitic pyroclastic rocks (lapilli tuff to tuff breccia), and lesser lenses of mudstone, limestone, and chert referred to as the ‘intermediate volcanic unit’ (IJHvc, Fig. 3) by Alldrick et al. (1986). Dacite-andesite flows to lapilli tuff to tuff breccia from this unit provided ages between 198 Ma and 193 Ma (Mortensen and Kirkham, 1992; Greig and Gehrels, 1995). This unit is broadly equivalent to the Unuk River andesite of the Betty Creek Formation as defined in the McTagg anticlinorium (Lewis, 2013; Gagnon et al., 2012; Nelson et al., 2018; Hunter and van Straaten, 2020).

At the base of the upper Hazelton Group is a unit of volcanic breccia, sandstone, conglomerate, lesser dacite and andesite flows, pyroclastic rocks, and minor siltstone and limestone that Alldrick et al. (1986) referred to as the ‘epiclastic and felsic volcanic unit’ (unit IJHsv, Fig. 3). The upper Hazelton Group pyroclastic and epiclastic rocks are inferred to record shallow-water sedimentation punctuated by gravity slide-generated mass flow (McCuaig and Sebert, 2017). Although this unit is predominantly andesitic (McCuaig and Sebert, 2017), the compositions range from basalt to rhyolite. A rhyolitic lapilli tuff collected from drill core at the Wolf deposit provided a LA-ICP-MS U-Pb zircon age of 178 ± 2.2 Ma. South of Kitsault Lake, a distinct horizon of epiclastic strata extends for ca. 5 km and is host to the Sault showing (Fig. 3). The horizon is a 20-100 m thick, northeast-trending, bedded zone of calcareous and locally graphitic sedimentary and felsic volcanoclastic rock that likely represents a hiatus in Hazelton Group volcanism. Overlying the ‘epiclastic and felsic volcanic unit’ is an ‘upper sedimentary unit’ of fossiliferous greywacke with belemnites and bivalves, black siltstone, sandstone, limestone, and arkose (Fig. 3; Alldrick et al., 1986). A volcanic-derived sandstone with belemnite casts provided a maximum deposition age of 168.9 ± 2.2 Ma (Hunter and van Straaten, 2020), which suggests the ‘upper sedimentary unit’ is likely a part of the

Quock Formation (Hunter and van Straaten, 2020). The Bowser Lake Group gradationally overlies the upper Hazelton Group strata and consists of interbedded siltstone, sandstone and chert-pebble conglomerate (Alldrick et al., 1986; Hunter and van Straaten, 2020).

4. Updated preliminary lithostratigraphy of the Hazelton Group

Below we update facies assignments used by Hunter and van Straaten (2020) and reconsider the stratigraphy proposed by Alldrick et al. (1986) for the Hazelton Group in the Kitsault area (Fig. 4, Table 1).

4.1. Lower Hazelton Group

4.1.1. Facies 1; Volcanic-derived sandstone, conglomerate, and mega-conglomerate

Based on detailed mapping by Miller et al. (2020), we redefine facies 1 (cf. Hunter and van Straaten, 2020; Table 1) the very basal unit of the Hazelton Group in the Kitsault River area (Fig. 4). It consists of massive to weakly stratified pebble to large boulder, polymictic conglomerate (Kinskuch conglomerate) with rounded to angular clasts, locally interbedded with and incised by coarse-grained feldspathic sandstone with lithic fragments and tuff (Fig. 5a; Miller et al., 2020). Clasts range up to 120 m and include sandstone, mudstone, limestone, chert, and volcanic rock-derived clasts of Stuhini Group augite-phyric basalt and Hazelton Group hornblende-plagioclase-phyric andesite (Miller et al., 2020). Maximum depositional ages yielded by U-Pb analysis of detrital zircons from a basal Hazelton Group volcanic-derived sandstone (228.4 ± 1.4 Ma) and a polymictic pebble conglomerate (206.7 ± 1.9 Ma), and a U-Pb zircon crystallization age from a porphyry diorite stock dated at 204.6 ± 0.18 Ma constrain facies 1 to the Rhaetian (Hunter and van Straaten, 2020; Miller et al., 2020).

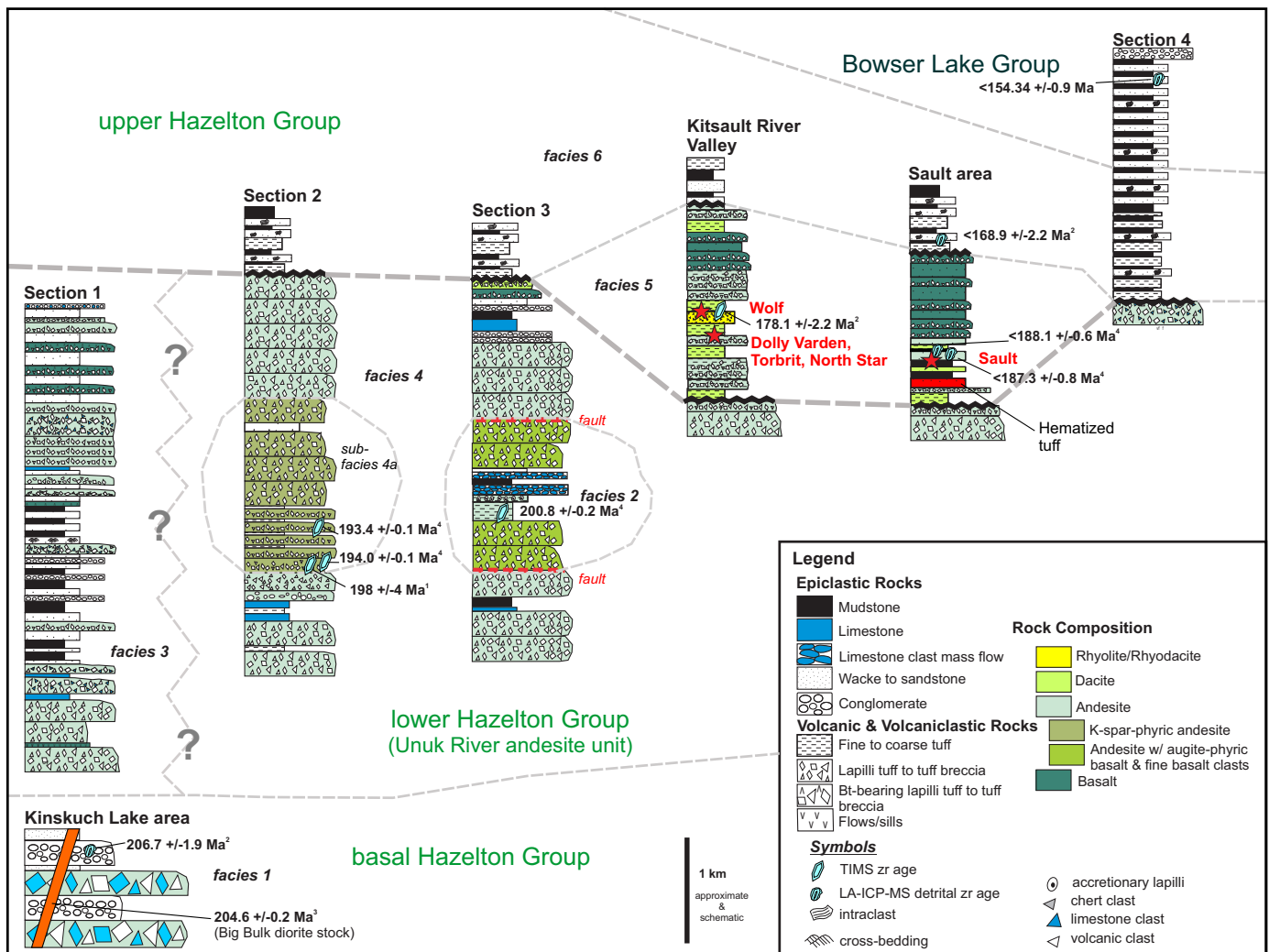


Fig. 4. Updated stratigraphy and lithostratigraphic correlations in the Kitsault River area. Sections are schematic composites compiled from map data. U-Pb zircon ages are from ¹Greig and Gehrels (1995), ²Hunter and van Straaten (2020), ³Miller et al. (2020), and ⁴this study. See Fig. 3 for locations.

4.1.2. Facies 2; Hornblende-plagioclase-phyric volcanic rocks, tuff, sandstone, conglomerate, and limestone

Facies 2 (redefined from facies 3 of Hunter and van Straaten, 2020; Table 1) is exposed along a prominent north-trending ridge between glacier-covered valleys 3.7 km east of Kinskuch Lake (Fig. 3). It consists of lapilli tuff, lapillistone, and tuff breccia, and rocks such as limestone, limestone clast-rich conglomerate, conglomerate, fine-grained sandstone, and mudstone (Figs. 4, 5b). The tuff breccias locally contain abundant augite-phyric basalt, and hornblende-plagioclase-phyric volcanic clasts. Although basal and upper contacts were not observed, the unit shares similarities to rocks described by Miller et al. (2020) that lie above the Kinskuch conglomerate. A tuff sample yielded an inferred depositional age of ca. 201 Ma (see below).

4.1.3. Facies 3; Hornblende-plagioclase-phyric pyroclastic and epiclastic facies

Facies 3 (grouped facies 1 and 2 in Hunter and van Straaten,

2020; Table 1) consists of poorly sorted lapilli tuff to tuff breccia with subrounded to subangular hornblende-plagioclase-phyric clasts, plus limestone and chert clasts in a hornblende-plagioclase-crystal-bearing matrix (Fig. 4). The lapilli tuff to tuff breccia is intercalated with extensive thick recessive beds of siltstone and fine-grained feldspathic sandstone in repeating fining-upward sequences with 10-50 m-thick micritic limestone, feldspathic sandstone, and conglomerate and rare chert (Fig. 5c). The facies contains local 50-100 m thick beds of biotite-bearing, matrix- to clast-supported lapilli tuff to tuff breccia with subrounded to subangular 3 mm to 10 cm biotite-plagioclase-phyric clasts in a biotite and plagioclase crystal-bearing matrix. A 5 m thick, coherent, augite-plagioclase-phyric unit is near the base of the unit.

4.1.4. Facies 4; hornblende-plagioclase-phyric volcanic facies

Facies 4 is a thick to very thick-bedded, hornblende-plagioclase lapilli tuff, lapillistone, tuff breccia and pyroclastic



Fig. 5. Representative photographs of facies 1, 2 and 3. **a)** Facies 1, Kinskuch conglomerate with grey limestone megaclast resting within irregularly interbedded coarse-grained sandstone and limestone-chert pebble conglomerate (UTM 475174E; 6170818N). **b)** Facies 2, clast-supported lapillistone with abundant accretionary lapilli (UTM 480620E; 6170990N). **c)** Facies 3, beds of clast- to matrix-supported polymictic conglomerate with rounded to subrounded clasts of chert, fine-grained tuff, and various plagioclase porphyritic fragments separated by a volcanic-derived sandstone layer (UTM 474247E; 6179466N). UTM: NAD 83, Zone 9.

breccia (Fig. 4). It contains subangular to subrounded, moderately to poorly sorted clasts that range from 0.4 to 60 cm in a fine- to coarse-ash matrix containing 2-5% hornblende and abundant plagioclase crystals (Fig. 6a). Volcanic clasts are predominant and consist of hornblende- and plagioclase-phyric (1-5 mm) fragments with varying phenocryst percentages (3-20%); aphyric volcanic and limestone clasts are local. The unit varies from matrix- to clast-supported and is massive to weakly graded. Locally, laterally discontinuous beds up to 2 m thick of graded coarse- to fine-tuff separate layers of lapilli tuff to tuff breccia. Locally interbedded with the polymictic lapilli tuff to tuff breccia are maroon, poorly sorted, thick-bedded, largely monomictic, matrix-supported lapilli tuff to tuff breccia with clasts that display ameoboid to wispy cusped-lobate clast boundaries.



Fig. 6. Lower Hazelton Group facies 4 rocks. **a)** Clast-supported lapillistone to lapilli tuff with subrounded to subangular hornblende-feldspar-phyric clasts with variable hornblende and plagioclase percentages (UTM 479119E; 6172627N). **b)** Hornblende-plagioclase-K-feldspar porphyry with zoned K-feldspar crystals up to 3 cm long aligned along bedding (UTM 479658E; 6175426N). UTM: NAD 83, Zone 9.

4.1.4.1. Sub-facies 4a; K-Feldspar and plagioclase porphyry and crystal tuff

Sub-facies 4a, originally placed in sub-facies 3a in Hunter and van Straaten (2020), is a distinct K-feldspar, hornblende, and plagioclase porphyry and crystal tuff exposed northeast of Kinskuch Lake and in a small (ca. 5 m) area north of Lavender Peak (Fig. 4). The unit varies from a massive, to flow-banded coherent rock, to plagioclase- and K-feldspar-bearing crystal tuff with K-feldspar crystals aligned along bedding (Fig. 6b; Hunter and van Straaten, 2020). The main exposure consists of a discontinuous unit that appears to be partially intercalated with facies 4 lapilli tuff to tuff breccia but contact relationships are obscured by weak to moderate disseminated sericite, limonite, and pyrite alteration. Zircons from a sub-facies 4a sample yielded a crystallization age of ca. 193 Ma (see below).

4.2. Upper Hazelton Group

4.2.1. Facies 5; Intermediate to mafic tuff, volcanic sandstone, local rhyolite to rhyolite tuff

Facies 5, in the Kitsault Valley and near the Sault showing ('intermediate volcanic unit' IJHvc of Fig. 3), consists of interbedded pyroclastic (tuff, lapilli tuff, crystal tuff, local tuff breccia) and more voluminous epiclastic sandstone to small pebble conglomerate (reworked tuff, lapilli tuff) with a combination of volcanic and sedimentary clast types (Figs. 4, 7a; McCuaig and Sebert, 2017). The unit is mainly andesitic but varies from basaltic to dacitic and locally, rhyolitic (McCuaig and Sebert, 2017). Minor rhyolites to rhyodacite tuffs are at the Wolf deposit and in the footwall of the Sault showing (McCuaig and Sebert, 2017). A rhyolitic lapilli tuff from the Wolf deposit yielded a preliminary CA-TIMS crystallization age of 178 ± 2.2 Ma (Hunter and van Straaten, 2020). The main basaltic section is exposed in the hanging wall of the Dolly Varden, Torbrit, North Star and Sault deposits and showings (McCuaig and Sebert, 2017). These basaltic rocks consist mainly of intercalated tuff and lapilli tuff to volcanic sandstone and conglomerate with variable amounts of volcanic-derived lithic clasts and vitric lapilli (Fig. 7b). The basaltic units appear to be discontinuous and their contacts with both the underlying volcanoclastic rocks and overlying sedimentary rocks have not been observed. Detrital zircons from a sandstone near the base of the section at the Sault showing yielded a maximum depositional age of ca. 187 Ma; another sample taken 50 m away yielded a maximum depositional age of ca. 188 Ma (see below). These comparatively young ages suggest that this sequence is in the upper Hazelton Group.

4.2.2. Facies 6; Interbedded feldspathic wacke, siltstone, tuff, minor black mudstone, limestone

Extensive, planar-bedded mudstone (locally black), siliceous siltstone, feldspathic wacke, limestone, and fine tuff to lapilli tuff is at the top of the Hazelton Group. The unit appears to have gradational contacts with underlying Hazelton Group volcano-sedimentary rocks and overlying Bowser Lake Group sedimentary rocks. The unit is distinguished by light-

brown weathering tuff beds that are 3-20 cm thick and consist of fine to coarse ash and 1-3 mm wispy lapilli. The tuff beds are intercalated with the mudstone-siltstone-sandstone beds (Fig. 7c) and decrease in number up section (Fig. 4). Local muddy limestone beds at the base of the unit contain rare belemnite casts. Detrital zircons from a sandstone near the southeast arm of Kitsault Lake (Fig. 3) yielded a preliminary maximum depositional age of 168.9 ± 2.2 Ma (Bajocian or younger; Hunter and van Straaten, 2020). Facies 6 is interpreted to be a part of the Quock Formation as described by Gagnon et al. (2012).

4.3. Bowser Lake Group

4.3.1. Interbedded feldspathic wacke, mudstone, and chert clast-bearing pebble conglomerate

Using criteria similar to Evenchick et al. (2010), the disappearance of facies 6 tuffaceous beds and the appearance of chert-pebble conglomerate are taken to mark the base of the Bowser Lake Group. In the Kitsault River area, the Bowser Lake Group consists of interbedded grey to brown, laminated- to medium-bedded, fine- to medium-grained feldspathic wacke and mudstone with local beds of chert-pebble conglomerate (Figs. 4, 7d). Load casts and flame structures are well developed, and 1-5 cm subrounded mudstone intraclasts are developed throughout the unit. The chert-pebble conglomerate forms metre-scale beds containing subrounded granules and pebbles in a coarse sandstone matrix. A sandstone sample yielded a maximum depositional age of ca. 154 Ma (see below).

5. Geochronology

Presented here are the analytical results from three Laser Ablation Inductively Coupled Plasma Mass Spectrometry (LA-ICPMS) and three Chemical Abrasion Thermal Ionization Mass Spectrometry (CA-TIMS) U-Pb zircon samples (Fig. 3). The samples, collected in 2019 and 2020, were analyzed at the Pacific Centre for Isotopic and Geochemical Research (The University of British Columbia). The complete analytical dataset for the CA-TIMS and LA-ICP-MS analyses will be presented elsewhere (Hunter et al., 2022).

5.1. Analytical procedures

5.1.1. LA-ICP-MS methods

Rock samples that underwent standard mineral separation procedures zircons were handpicked in alcohol and mounted in epoxy, along with reference materials. Grain mounts were wet ground with carbide abrasive paper and polished with diamond paste. Cathodoluminescence (CL) imaging was carried out on a Philips XL-30 scanning electron microscope (SEM) equipped with a Bruker Quanta 200 energy-dispersion X-ray microanalysis system at the Electron Microbeam/X-Ray Diffraction Facility (EMXDF) at the University of British Columbia. An operating voltage of 15 kV was used, with a spot diameter of 6 μm and peak count time of 17-27 seconds. After removal of the carbon coat the grain mount surface was washed with mild soap and rinsed with high purity water. Before

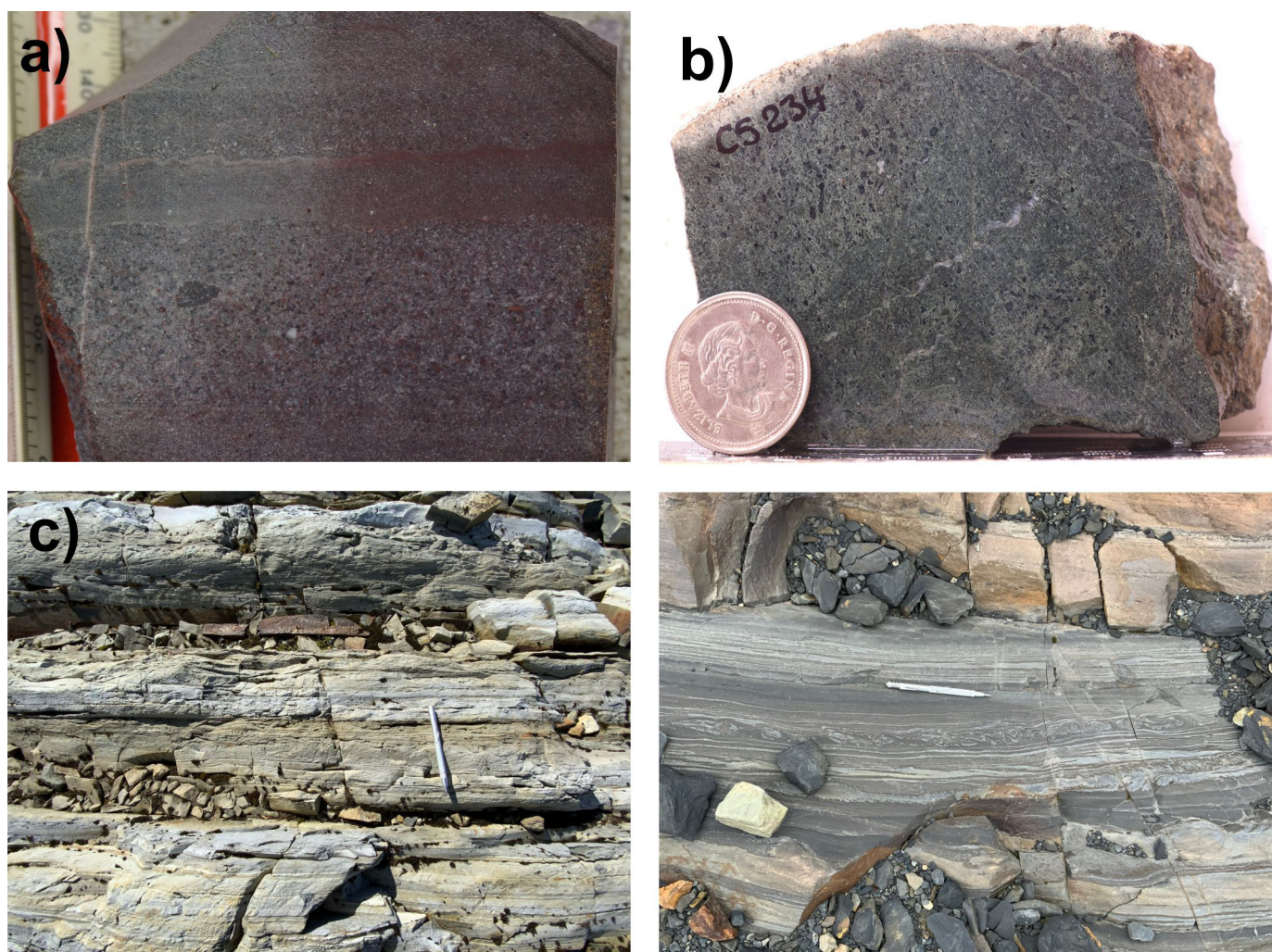


Fig. 7. Representative photos of upper Hazelton Group and Bowser Lake Group units. **a)** Facies 5, well-bedded, fine to very coarse-grained epiclastic sandstone with small volcanic-derived pebbles northwest of the Wolf deposit (UTM 467281E; 6173275N). **b)** Facies 5, dark green mafic lapilli tuff with pebble-sized glassy and weakly amygdaloidal clasts in a crystal- and ash-rich matrix (UTM 467801E; 6178200N). **c)** Facies 6, interbedded fine and coarse tuff (UTM 462065E; 6159694N). **d)** Bowser Lake Group, finely interlayered mudstone and siltstone (dark toned) and fine-grained sandstone (light toned) with soft-sediment deformation (UTM 463493E; 6183729N). UTM: NAD 83, Zone 9.

analysis the grain mount surface was cleaned with 3 N HNO₃ acid and again rinsed with high purity water to remove any surficial Pb contamination that could interfere with the early portions of the spot analyses.

Analyses were conducted using a Resonetics RESOLUTION M-50-LR, which contains a Class I laser device equipped with a UV excimer laser source (Coherent COMPex Pro 110, 193 nm, pulse width of 4 ns) and a two-volume cell designed and developed by Laurin Technic Pty. Ltd. (Australia). This sample chamber allowed investigating several grain mounts in one analytical session. The laser path was fluxed by N₂ to ensure better stability. Ablation was carried out in a cell with a volume of approximately 20 cm³ and a He gas stream that ensured better signal stability and lower U-Pb fractionation (Eggins et al., 1998). The laser cell was connected via a Teflon squid to an Agilent 7700x quadrupole ICP-MS housed at PCIGR. A pre-ablation shot was used to ensure that the spot area on grain surface was contamination-free. Samples

and reference materials were analyzed for 36 isotopes: ⁷Li, ²⁹Si, ³¹P, ⁴³Ca, ⁴⁵Sc, ⁴⁹Ti, Fe (⁵⁶Fe, ⁵⁷Fe), ⁸⁹Y, ⁹¹Zr, ⁹³Nb, ⁹⁵Mo, ⁹⁸Mo, ¹³⁹La, ¹⁴⁰Ce, ¹⁴¹Pr, ¹⁴⁶Nd, ¹⁴⁷Sm, ¹⁵³Eu, ¹⁵⁷Gd, ¹⁵⁹Tb, ¹⁶³Dy, ¹⁶⁵Ho, ¹⁶⁶Er, ¹⁶⁹Tm, ¹⁷²Lu, ¹⁷⁷Hf, ¹⁸¹Ta, ²⁰²Hg, Pb (²⁰⁴Pb, ²⁰⁶Pb, ²⁰⁷Pb, ²⁰⁸Pb), ²³²Th, and U (²³⁵U, ²³⁸U) with a dwell time of 0.02 seconds for each isotope. Pb/U and Pb/Pb ratios were determined on the same spots along with trace element concentration determinations. These isotopes were selected based on their relatively high natural abundances and absence of interferences. The settings for the laser were: spot size of 34 μm with a total ablation time of 30 seconds, frequency of 5 Hz, fluence of 5 J/cm², power of 7.8 mJ after attenuation, pit depths of approximately 15 μm, He flow rate of 800 mL/min, N₂ flow rate of 2 mL/min, and a carrier gas (Ar) flow rate of 0.57 L/min.

Reference materials were analyzed throughout the sequence to allow for drift correction and to characterize downhole fractionation for Pb/U and Pb/Pb isotopic ratios. For trace

elements, NIST 612 glass was used for both drift correction and trace element calibration, with sample spacing between every five to eight unknowns, and ^{90}Zr was used as the internal standard assuming stoichiometric values for zircon. NIST 610 glass was analyzed after each NIST 612 analysis and used as a monitor reference material for trace elements. For U-Pb analyses, natural zircon reference materials were used, including Plešovice (Sláma et al., 2008; 337.13 ± 0.33 Ma) or 91500 (Wiedenbeck et al., 1995; 2004; 1062.4 ± 0.4 Ma, $^{206}\text{Pb}/^{238}\text{U}$ date) as the internal reference material, and both Temora2 (Black et al., 2004; 416.78 ± 0.33 Ma) and Plešovice and/or 91500 as monitoring reference materials; the zircon reference materials were placed between the unknowns in a similar fashion as the NIST glasses. Raw data were reduced using the Iolite 3.4 extension (Paton et al., 2011) for Igor Pro™ yielding concentration values, Pb/U and Pb/Pb dates, and their respective propagated uncertainties. For all LA-ICPMS analyses, we excluded individual grain ages with <0.05 probability of concordance (calculated using the Isoplot routine of Ludwig, 2012). We calculated preliminary maximum depositional ages for detrital zircon samples using the youngest statistical population (YSP) in a probability density plot (PDP) constructed in Isoplot (Ludwig, 2012), which follows the methods of Herriott et al. (2019).

5.1.2. CA-TIMS methods

CA-TIMS procedures described here are modified from Mundil et al. (2004), Mattinson (2005) and Scoates and Friedman (2008). After rock samples underwent standard mineral separation procedures, zircons were handpicked in alcohol. The clearest, crack- and inclusion-free grains were selected, photographed and then annealed in quartz glass crucibles at 900°C for 60 hours. Selected individual annealed grains are transferred into clean 300 mL PFA microcapsules (crucibles) and ultrapure HF (up to 50% strength, 500 mL) and HNO_3 (up to 14 N, 50 mL) were added for chemical abrasion leaching step. They were placed in 125 mL PTFE liners (up to 15 per liner) and about 2 mL HF and 0.2 mL HNO_3 of the same strength as acid in beakers containing samples were added to the liners. The liners were then slid into stainless steel Parr™ high pressure dissolution devices, which were sealed and brought up to a maximum of 190°C for 8-16 hours (typically 175°C for 12 hours). Beakers are removed from liners and zircon is separated from leachate. Zircons were rinsed with >18 M Ω .cm water and sub-boiled acetone. Then 200 mL of sub-boiled 6N HCl was added and beakers were set on a hotplate at 80 - 130°C for 30 minutes and again rinsed with water and acetone. Masses were estimated from the dimensions (volumes) of grains. For full dissolution in same microcapsules (crucibles), about 50 mL 50% HF and 5 mL 14 N HNO_3 were added and each was spiked with a $^{233-235}\text{U}$ - ^{205}Pb tracer solution (EARTHTIME ET535), capped and again placed in a Parr liner (up to 15 microcapsules per liner). HF and nitric acids in a 10:1 ratio, respectively, were added to the liner, which was then placed in Parr high pressure device and dissolution was achieved at 220°C for 40 hours.

The resulting solutions were dried on a hotplate at 130°C , 50 mL 6N HCl was added to microcapsules and fluorides were dissolved in high pressure Parr devices for 12 hours at 180°C . HCl solutions were transferred into clean 7 mL PFA beakers and dried with 2 mL of 0.5 N H_3PO_4 . Samples were loaded onto degassed, zone-refined Re filaments in 2 mL of silicic acid emitter (Gerstenberger and Haase, 1997).

Isotopic ratios were measured with single collector VG 54R thermal ionization mass spectrometers equipped with analogue Daly photomultipliers. Analytical blanks were 0.1 pg for U and up to 1 pg for Pb. U fractionation was determined directly on individual runs using the EARTHTIME ET535 mixed $^{233-235}\text{U}$ - ^{205}Pb isotopic tracer and Pb isotopic ratios were corrected for fractionation of $0.40 \pm 0.04\%$ /amu, based on replicate analyses of NBS-982 reference material and the values recommended by Thirlwall (2000). Data reduction employed the excel-based program of Schmitz and Schoene (2007). Unless otherwise noted all errors were quoted at the 2 sigma or 95% level of confidence. Isotopic dates are calculated with the decay constants $\lambda_{238} = 1.55125\text{E-}10$ and $\lambda_{235} = 9.8485\text{E-}10$ (Jaffe et al., 1971) and a $^{238}\text{U}/^{235}\text{U}$ ratio of 137.88. EARTHTIME U-Pb synthetic solutions were analyzed on an on-going basis to monitor the accuracy of results. Standard concordia diagrams were constructed and regression intercepts, weighted averages calculated with Isoplot (Ludwig, 2003; 2012).

5.2. Results

5.2.1. Sample 19RHU-10-2a, fine tuff from facies 2 (CA-TIMS)

The sample from facies 2 was collected 3.7 km east of Kinskuch Lake along a prominent outcrop ridge with almost near continuous exposure (Fig. 3). The sample is from an 8.5 m thick fine tuff that is interbedded with coarse tuff on the mm- to cm-scale (Fig. 8a). This unit is conformably underlain and overlain by m-scale beds of muddy limestone to calcareous mudstone, medium-grained sandstone, as well as tuff, lapilli tuff (locally containing accretionary lapilli) and tuff breccia locally containing augite-phyric and basalt clasts. Nineteen anhedral to subhedral zircons were extracted from the sample and five of these were selected for CA-TIMS analysis. They range in size from 100 to 150 μm and have 1:2 aspect ratios. Out of the five analyzed zircons, one provided a $^{206}\text{Pb}/^{238}\text{U}$ date of $201.24 \text{ Ma} \pm 0.24 \text{ Ma}$ and is inferred to be a xenocryst or antecryst. The remaining four grains overlap on concordia (Fig. 9a) and have a weighted mean $^{206}\text{Pb}/^{238}\text{U}$ age of $200.85 \pm 0.15 \text{ Ma}$ (MSWD=1.63), which is inferred to be the depositional age of the tuff (Fig. 9b).

5.2.2. Sample 19RHU-1-1, potassium feldspar-phyric andesite from sub-facies 4a (CA-TIMS)

Sample 19RHU-1-1 was collected from sub-facies 4a northeast of Kinskuch Lake (Fig. 3). It is a coherent, medium-grained andesite and consists primarily of plagioclase, 3% hornblende and 2-3% potassium feldspar phenocrysts between 1 and 3 cm in size (Fig. 8b). It surrounded by m-scale beds

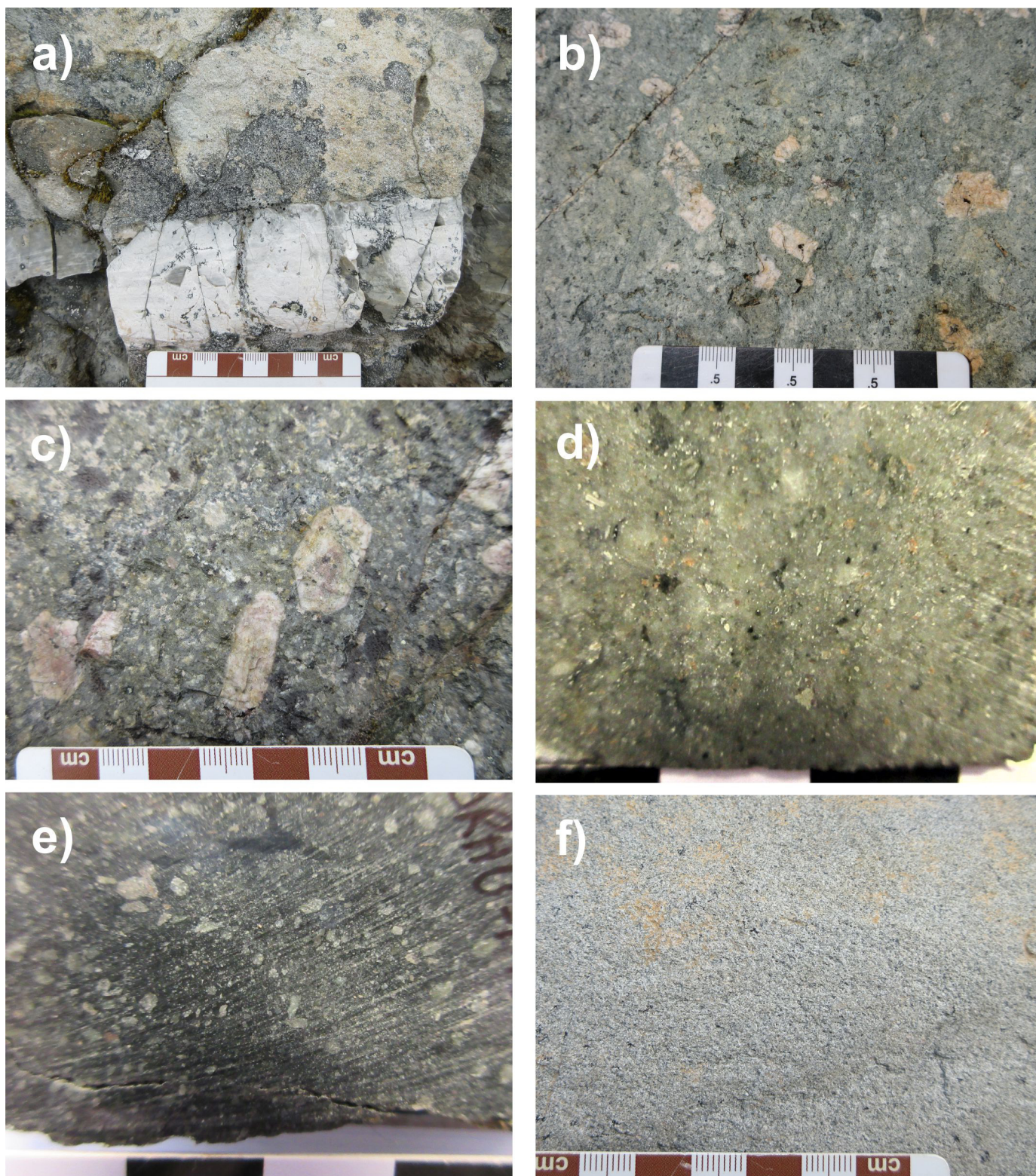


Fig. 8. Photographs of geochronological samples. **a)** Facies 2, sample 19RHU-10-2a, white weathering fine tuff bed interbedded with coarse to fine lapilli tuff (UTM 480620E; 6170990N). **b)** Sub-facies 4a sample 19RHU-1-1, massive, K-feldspar-plagioclase-hornblende-phyric andesite porphyry with cm phenocrysts of K-feldspar (UTM 479953E; 6175692N). **c)** Sub-facies 4a sample 19RHU-4-2, same as above with K-feldspar phenocrysts up to 3 cm long (UTM 478931E; 6175118N). **d)** Facies 5 sample 20RHU-1-14, light green, crystal tuff to lapilli tuff with 1-3 mm black vitric lapilli (UTM 469159E; 6178502N). **e)** Facies 5 sample 20RHU-1-16, dark gray, poorly-sorted, graphitic fine-grained sandstone with 2-3 mm blocky plagioclase fragments and irregular 1-3 mm dark gray vitric clasts (UTM 469160E; 6178519N). **f)** Bowser Lake Group sample 19RHU-16-1, white weathering, coarse-grained feldspathic wacke (UTM 485465E; 6171061N). UTM: NAD 83, Zone 9.

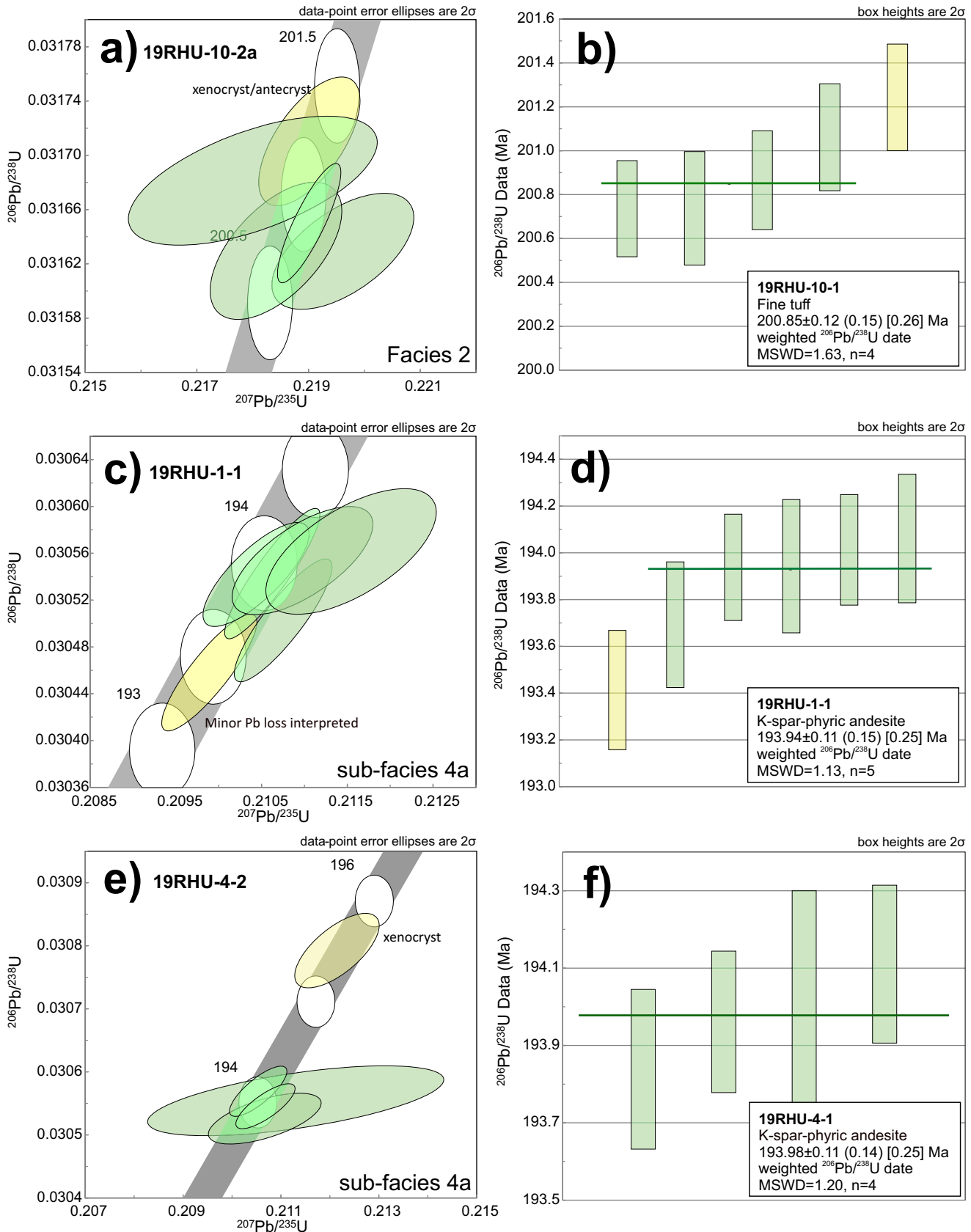


Fig. 9. CA-TIMS analyses plots of zircons. **a)** Concordia plot of zircons from sample 19RHU-10-2a. **b)** $^{206}\text{Pb}/^{238}\text{U}$ ages and calculated mean age for sample 19RHU-10-2a. **c)** Concordia plot of zircons from sample 19RHU-1-1. **d)** $^{206}\text{Pb}/^{238}\text{U}$ ages and calculated mean age for sample 19RHU-1-1. **e)** Concordia plot of zircons from sample 19RHU-4-2. **f)** $^{206}\text{Pb}/^{238}\text{U}$ ages and calculated mean age for sample 19RHU-4-2.

of lapilli tuff to tuff breccia with hornblende-plagioclase-phyric fragments. The contact area varies from abrupt with overprinting strong limonite and sulphide alteration, and in other localities, the porphyry appears gradational and transitions into a potassium-feldspar-phyric lapilli tuff to tuff breccia. Forty-one subhedral to euhedral zircons were extracted from the sample and six of these were selected for CA-TIMS analysis. The zircons are 100 to 200 μm in length with 1:1 to 1:2 aspect ratios. Five of six grains analyzed are mutually overlapping on concordia and yield a weighted mean $^{206}\text{Pb}/^{238}\text{U}$ age of 193.93 ± 0.11 Ma (MSWD=1.13), which is interpreted to be the crystallization age of the sample (Figs. 9c, d). A single zircon overlaps concordia with a slightly younger $^{206}\text{Pb}/^{238}\text{U}$ date of 193.42 ± 0.11 Ma, is inferred to have undergone minor Pb loss (Fig. 9c).

5.2.3. Sample 19RHU-4-2, potassium feldspar-phyric andesite from sub-facies 4a (CA-TIMS)

A second potassium-feldspar-phyric andesite was collected from sub-facies 4a northeast of Kinskuch Lake (Fig. 3). It is a coherent andesite and contains 3-5%, 1-4 cm phenocrysts of potassium feldspar in a plagioclase-rich groundmass with 3% hornblende (Fig. 8c). The andesite is adjacent to hornblende-plagioclase-phyric andesite lapilli tuff to tuff breccia, but contact relationships are obscured by moderate limonite and sulphide alteration. Thirty-nine subhedral to euhedral zircons were extracted from the sample having sizes between 100 and 200 μm and 1:2 to 1:3 aspect ratios. Five zircons were selected for CA-TIMS analysis. One grain overlaps concordia with an older $^{206}\text{Pb}/^{238}\text{U}$ date of 195.51 ± 0.30 Ma and is inferred to be a xenocryst (Fig. 9e). Four grains are mutually overlapping on concordia and provide a weighted mean $^{206}\text{Pb}/^{238}\text{U}$ age of 193.98 ± 0.11 Ma (MSWD=1.20), which is interpreted to be the crystallization age of the sample (Fig. 9f).

5.2.4. Sample 20RHU-1-14, volcanic sandstone from facies 5 (LA-ICPMS)

From facies 5, this sample was collected 600 m south of Kitsault Lake (Fig. 3). It is from a light green, weakly foliated, clast-supported, carbonaceous volcanic sandstone with subangular plagioclase and crystal tuff fragments near the base of the section at the Sault showing (Fig. 8d). Zircon grains are largely subrounded, partially fragmented, and have aspect ratios of 1:1 to 1:2, with long dimensions ranging from 100-200 μm . Most $^{206}\text{Pb}/^{238}\text{U}$ dates span ca. 178-212 Ma (n=108) with a single primary peak at 191 Ma; two older zircons have $^{206}\text{Pb}/^{238}\text{U}$ dates of ca. 361 Ma and 373 Ma (Fig. 10a). The youngest statistical population provided a mean age of 187.33 ± 0.83 Ma (MSWD=1.00; n=31), which is interpreted to be the maximum depositional age (Fig. 10b).

5.2.5. Sample 20RHU-1-16, graphitic, calcareous volcanic sandstone from facies 5 (LA-ICPMS)

The facies 5 sample was also collected south of Kitsault Lake, 17 m north of 20RHU-1-14 (Fig. 3). It is a graphite-

bearing, calcareous, poorly sorted, volcanic sandstone with 1-3 mm subangular clasts of plagioclase and plagioclase crystal tuff and lesser black wispy vitric fragments (Fig. 8e). It has a moderate foliation defined by graphite. Zircon grains are mainly subrounded, fragmented to subhedral, and have aspect ratios of 1:1 to 3:1, with long dimensions varying from 100-250 μm . Most $^{206}\text{Pb}/^{238}\text{U}$ dates span 203.4-182.7 Ma (n=103) with a broad age peak defined at 190.0 Ma (Fig. 10c). The youngest statistical population yielded a mean age of 188.08 ± 0.59 Ma (MSWD=0.99; n=61), which is interpreted to be the maximum depositional age (Fig. 10d).

5.2.6. Sample 19RHU-16-1, feldspathic wacke from Bowser Lake Group (LA-ICPMS)

This feldspathic wacke sample was taken from the Bowser Lake Group, 8.5 km east of Kinskuch Lake (Fig. 3). It is from a section of fine- to medium-grained feldspathic wacke and very fine-grained, laminated, graphite-bearing gray to black siltstone interbedded on the 0.5 to 1 m scale (Fig. 8f). The sample has three distinct $^{206}\text{Pb}/^{238}\text{U}$ probability peaks spanning the Late Triassic to Late Jurassic at ca. 197 Ma, 187 Ma, and 156 Ma (Fig. 10e). One concordant zircon provided a Carboniferous $^{206}\text{Pb}/^{238}\text{U}$ date at ca. 306 Ma. The youngest statistical population provided a mean age of 154.31 ± 0.93 Ma (MSWD=1.00; n=16), which is interpreted to be the maximum depositional age (Fig. 10f). This age is well within the Bowser Lake Group time frame.

6. Discussion

6.1. Lithostratigraphic and geochronological considerations

As documented previously, a maximum depositional age of 206.7 ± 1.4 Ma (Hunter and van Straaten, 2020) and a crystallization age of 204.6 ± 0.18 Ma (Miller et al., 2020) indicate that the onset of Hazelton Group deposition was during the Rhaetian and that deposition of facies 1 was coeval with or older than facies 2. Rocks that Alldrick et al. (1986) referred to as the 'middle sedimentary unit' appear to form the basal Hazelton Group (facies 1 and 2) and rocks of the 'intermediate volcanic unit' are more accurately placed in the lower Hazelton Group (facies 3 and 4; i.e., part of the Betty Creek Formation-Unuk River andesite unit; Table 1). The 'epiclastic and felsic volcanic unit' of Alldrick et al. (1986) is problematic because the main exposures east of Kinskuch Lake and northwest of the Kitsault River Valley (Fig. 3) are largely intermediate volcanoclastic rocks of facies 4 with local exposures of predominantly epiclastic units similar to units found in facies 3. We therefore interpret that the 'epiclastic and felsic volcanic unit' defined by Alldrick et al. (1986) does not form a discrete unit that can be mapped consistently across the area.

The fine tuff sampled within facies 2 provided a crystallization age of 200.9 ± 0.2 Ma (Hettangian) and indicates that it is older than the thick ca. 193 Ma (Facies 4, sub-facies 4a) andesitic units and is younger than the inferred age of the basal Hazelton Group. It is interbedded with abundant limestone, as well as augite-phyric tuff breccia, which further suggests that this unit

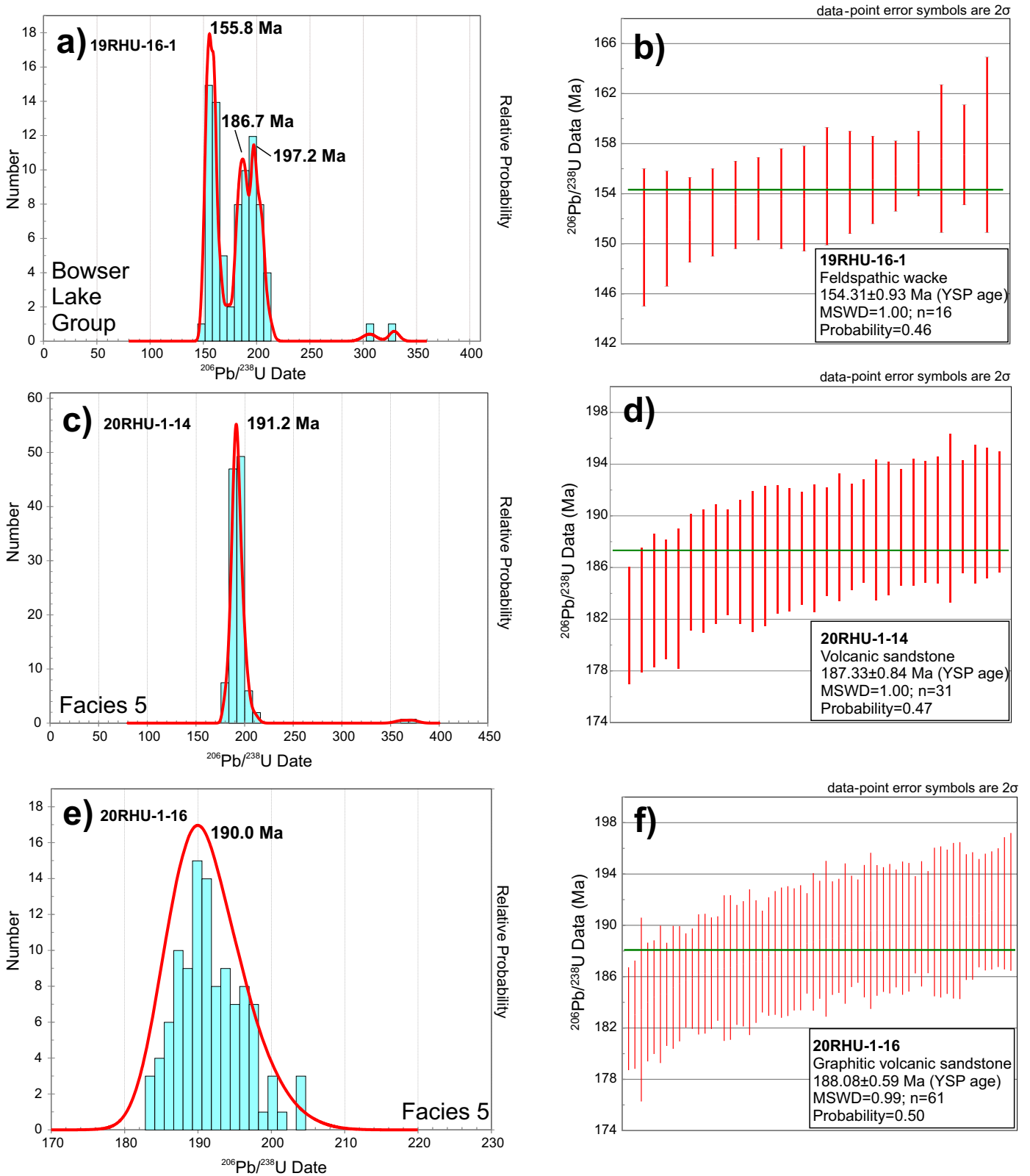


Fig. 10. LA-ICP-MS analyses plots of zircons. **a)** $^{206}\text{Pb}/^{238}\text{U}$ probability density plot showing the main probability age peaks for sample 19RHU-16-1. **b)** $^{206}\text{Pb}/^{238}\text{U}$ ages and calculated mean age for the youngest statistical population for sample 19RHU-16-1. **c)** $^{206}\text{Pb}/^{238}\text{U}$ probability density plot from showing the main probability age peaks for sample 20RHU-1-14. **d)** $^{206}\text{Pb}/^{238}\text{U}$ ages and calculated mean age for the youngest statistical population for sample 20RHU-1-14. **e)** $^{206}\text{Pb}/^{238}\text{U}$ probability density plot from showing the main probability age peaks for sample 20RHU-1-16. **f)** $^{206}\text{Pb}/^{238}\text{U}$ ages and calculated mean age for the youngest statistical population for sample 20RHU-1-16.

likely represents more of the basal Hazelton Group deposited before the thick andesitic pyroclastic flows of facies 4 that make up the bulk of the lower Hazelton Group. The ridge that these rocks are exposed along could represent a localized upthrown block of the basal Hazelton group east of Kinskuch Lake. Thus far, the basal Hazelton Group contact with the Stuhini Group in the Kitsault area appears much more gradational and contrasts to the sharp, inferred erosional contacts observed in the Snippaker area and the McTagg anticlinorium (Nelson and Kyba, 2014; Kyba and Nelson, 2015). Because facies 1 and 2 represent a unique and mappable lithostratigraphic unit, we suggest that together they form part what we refer to as the 'Kinskuch unit', which includes the 'Kinskuch conglomerates' of Miller et al. (2020; Table 1).

Facies 3 consists of abundant hornblende-plagioclase-phyric andesite interbedded with epiclastic rocks (limestone, siltstone, sandstone, conglomerate). The pyroclastic rocks also contain abundant limestone and chert clasts, in contrast to facies 4, which contains almost entirely volcanic-derived clasts. Although the age of facies 3 has not been determined, a U-Pb zircon age of 193.5 ± 0.4 Ma was obtained from a felsic volcanic unit below the Sault showing (Mortensen and Kirkham, 1992) that could be a part of facies 3. Accordingly, facies 3 may be laterally equivalent to facies 4 and represent sedimentation in a relatively deep-marine setting distal to the main eruption centre(s). Alternatively, if the dated felsic volcanic unit is not apart of facies 3, then it could either be younger than facies 4 and represent an interim period between basal Hazelton sedimentation and the deposition of the thick andesitic pyroclastic flows of facies 4, or older and represent a gradual shift of facies 3 to more epiclastic sedimentation as the andesitic volcanism waned. Two K-feldspar-phyric andesite samples from Facies 4a have crystallization ages at ca. 193 Ma, placing facies 4 within the age range of the Unuk River andesite unit of the Betty Creek Formation (Gagnon et al., 2012; Nelson et al., 2013). The very coarse-grained K-feldspar megacrysts and locally massive texture indicate that facies 4a may represent feeder sub-volcanic intrusions to volcanism responsible for the thick andesitic lapilli tuff to tuff breccia rocks of Facies 4. Alternatively, the plagioclase and K-feldspar-phyric sub-facies 4a may represent intrusions similar to the Premier diorite to monzonite intrusions (Febbo et al., 2015) that host the Au-Cu porphyry Mitchell and Sulphurets deposits. U-Pb zircon ages from diorite plutons with K-feldspar phenocrysts in the Sulphurets suite have similar Lower Jurassic ages of 196 ± 2.9 Ma, 192.2 ± 2.8 Ma and 189 ± 2.8 Ma (Febbo et al., 2015).

Near the Sault showing, two epiclastic samples from facies 5 provided similar ca. 188 Ma maximum depositional ages. The epiclastic strata are underlain by feldspar-phyric lapilli tuff inferred to be facies 3 or 4 that have been loosely dated at ca. 196 Ma and ca. 193 Ma (Fig. 3; Mortensen and Kirkham, 1992; Greig and Gehrels, 1995). The difference in age may indicate a significant break in sedimentation from the Sinemurian (facies 3 and 4 lapilli tuff) to the Pleinsbachian

or younger (facies 5 epiclastic units) in the Sault showing area. The abundance of carbonate rocks in units at the Sault showing could suggest equivalence to the Spatsizi Formation, which is distributed throughout the Stewart-Iskut district. The remaining pyroclastic to epiclastic strata of facies 5 are not documented elsewhere in the Stewart-Iskut district and are unlike rocks of the Iskut River Formation, which host large VMS-type mineralization systems. We suggest that facies 5 constitutes a new mappable lithostratigraphic unit, referred to as the 'Kitsault unit' in Table 1, and that it forms part of the upper Hazelton Group outside of the main Eskay rift.

6.2. Implications for Kitsault River area mineralization systems and expression of VMS and VMS-related mineralization external to the main Eskay rift

The Kitsault River area hosts numerous stratabound to vein infill Ag-rich Pb-Zn deposits and showings such as Dolly Varden, Torbrit, North Star, Wolf, and Sault (Hanson, 1922; Black, 1951; Campbell, 1959; Dawson and Alldrick et al., 1986; Devlin and Godwin, 1986; Pinsent, 2001; Dunn and Pinsent, 2002), which have been interpreted variously as: epithermal vein-related (Grove, 1986); stratabound VMS (Devlin and Godwin, 1985; Devlin, 1987); shallow subaqueous hot spring (Dunn and Pinsent, 2002); or hybrid VMS-epithermal (Hunter and van Straaten, 2020). Additional descriptions of the Dolly Varden, Torbrit, North Star and Wolf deposits can be found in Hunter and van Straaten (2020). The deposits and showings are along, or peripheral to major northwest- and northeast-trending faults with inferred normal and strike-slip movement (Devlin and Godwin, 1986; McCuaig and Sebert, 2017).

The Sault showing is a small exhalative zone that is thought to be broadly correlative to the Dolly Varden deposits (McCuaig and Sebert, 2017). It consists of stratiform Zn-Pb-Ag-Sr mineralization that forms disrupted laminae of pyrite, sphalerite, celestite, and galena at the base of an approximately 50 m thick calcareous and locally graphitic sedimentary to volcanoclastic section consisting of interbedded mudstone, sandstone, muddy limestone, chert, and tuff to fine lapilli tuff layers, including a unit described as a metalliferous carbonate diamictite (Tupper and McCartney, 1990; Mortensen and Kirkham, 1992; Pinsent, 2001). The showing is overlain by a basaltic to andesitic tuffaceous rock with minor epiclastic beds and underlain by andesitic lapilli tuff to tuff breccia with local epiclastic sequences (Tupper and McCartney, 1990). The best mineralized diamond drill hole intersection contained 1.3% Zn, 0.12% Pb, 26.5 g/t Ag and 10 ppb Au along 4.95 m coincident with fault rock and minor carbonate and quartz veins (Tupper and McCartney, 1990). Alteration associated with the mineralized zones consist of ankerite, silica, pyrite and weak sericite and clay (Tupper and McCartney, 1990).

The ca. 178 Ma felsic tuffaceous sandstone dated at Wolf (Hunter and van Straaten, 2020), shows that at least some of the mineralization in the Kitsault River area is cogenetic with VMS deposits in the upper part of the Hazelton Group elsewhere, such as at Eskay Creek and Anyox (Alldrick, 1993; Smith,

1993; Barrett and Sherlock, 1996; Evenchick and McNicoll, 2002; MacDonald et al., 1996a; Macdonald et al., 1996b; Roth et al., 1999; Sherlock et al., 1999; Barresi and Dostal, 2005). In contrast, the new maximum depositional age of ca. 188 Ma for epiclastic rocks at the Sault showing could indicate that some of the Ag-rich mineralization systems are slightly older.

The Eskay Creek deposit encompasses several stratiform to discordant Au-Ag-Pb-Zn-Cu zones with disseminated, massive to semi-massive sulphides and sulphosalts with varying amounts of barite (Sherlock et al., 1999) and is inferred to have formed as shallow-water VMS or as a hybrid VMS-epithermal system (Roth et al., 1999; Galley et al., 2007) with bimodal volcanism (Barrie and Hannington, 1999; Franklin et al., 2005). The Ag-rich nature of the Kitsault River area deposits, which lack significant Au enrichment, is unique. Higher Ag and Pb values in VMS settings are generally in areas that host more sedimentary rocks, such as the bimodal-siliciclastic VMS-type (Barrie and Hannington, 1999; Franklin et al., 2005; Hannington et al., 2005). However, the Kitsault River area lacks significant turbiditic deposits. In contrast to the Besshi deposits in Japan or Windy Craggy in British Columbia (Peter and Scott, 1999), the Kitsault deposits are hosted largely in intermediate to dacitic epiclastic to fine pyroclastic rocks between a lower package of andesitic lapilli tuff to tuff breccia and an upper package of calc-alkaline fine-grained mafic pyroclastic rocks.

Coupled with Ag-rich mineralization, the lithologic characteristics of the Kitsault area suggest that it either represents a new, underexplored VMS deposit type or a hybrid VMS-epithermal system. Other Au-Ag-rich VMS-type mineralization in late Early to Middle Jurassic Hazelton Group rocks includes new discoveries southeast of the Brucejack Mine (Pretium Resources Inc., 2021; Brueckner et al., 2021), north of the Premier deposit at Silver Hill (Ascot Resources Ltd., 2020), and 30 km northeast of Stewart at Todd Creek (ArcWest Exploration Inc., 2019). These examples demonstrate the vast VMS-type mineralization potential of the Hazelton Group outside of the traditional Eskay rift. Additional bedrock mapping, targeted age dating and geochemical analysis will be vital to understand the upper Hazelton Group and its prospectivity for these new or hybrid VMS mineralization systems.

7. Conclusions

Updating the pioneering stratigraphic assignments in the Kitsault area by Alldrick et al. (1986), we divide the Hazelton Group into six facies and one sub-facies. Facies 1, with maximum depositional ages of ca. 206–204 Ma, consists of volcanic-derived sandstone, conglomerate, and megaclast-bearing conglomerate that forms the basal part of the lower Hazelton Group. Facies 2 comprises augite- and hornblende-plagioclase-phyric volcanic rocks, tuff, sandstone, conglomerate, and limestone. A fine tuff within this facies has a depositional age of 200.9 ± 0.2 Ma making it slightly younger than the basal Hazelton Group. Facies 1 and 2 form part of a lithostratigraphic unit that we refer to as the ‘Kinskuch

unit’. Facies 3 consists of hornblende-plagioclase-phyric pyroclastic rocks with significant exotic clasts (limestone, chert), and interbedded siltstone, sandstone, conglomerate, and limestone. Facies 4 is mainly lapilli tuff to tuff breccia containing volcanic-derived, hornblende-plagioclase-phyric clasts with minor tuff, sandstone, and limestone interbeds. Two samples of K-feldspar porphyry (sub-facies 4a) to flow-banded tuff within Facies 4 yielded ca. 193 Ma crystallization ages. Facies 3 is inferred to be slightly younger, slightly older, or a distal equivalent to facies 4. The upper Hazelton Group begins with facies 5 and consists mainly of mafic to intermediate tuff, volcanic sandstone, and dacite to dacite tuff. The age of facies 5 is constrained by maximum depositional ages of ca. 188 Ma for volcanic sandstone units from the Sault showing and a ca. 178 Ma rhyolite lapilli tuff from the Wolf deposit. Facies 5 forms part of a newly named lithostratigraphic unit we refer to as the ‘Kitsault unit’ and likely localized expressions of the Spatsizi Formation. With a maximum deposition age of ca. 168 Ma, facies 6 consists of interbedded feldspathic wacke and fine lapilli tuff to tuff with lesser limestone and black mudstone. Facies 6 grades into interbedded feldspathic wacke, mudstone and chert clast-bearing pebble conglomerate of the Bowser Lake Group, with a maximum depositional age of ca. 154 Ma. Preliminary stratigraphic and geochronological results suggest that VMS type mineralization in the Kitsault River area has a potential age range from ca. 188 to ca. 178 Ma, which may indicate that the mineralization systems could be older than the Au-rich VMS systems in the Eskay rift. Future mapping-based studies in the Kitsault River area will be vital to better resolve the stratigraphy, timing, and geochemistry of the Hazelton Group and its important mineralizing systems.

Acknowledgments

We thank Dolly Varden Silver Corporation, in particular Rob van Egmond, Amanda Bennett, and Charlie Fleenor, for their logistical support, and their hospitality while we stayed in the Alice Arm Camp. We thank Summit Helicopters and their pilots for getting us out to and back from the field throughout the summer. Emily Miller is thanked for the use of some of her M.Sc. thesis photos and information. Cheerful and dedicated field assistance was provided by Ben Coats. Hai Lin, Taylor Ockerman and Marghalera Animi are thanked for their work in preparation and analysis of the geochronological samples. Insightful reviews by JoAnne Nelson, Jeff Chiarenzelli, and Lawrence Aspler significantly improved this manuscript.

References cited

- Anderson, R.G., 1989. A stratigraphic, plutonic and structural framework for the Iskut map area, northwestern British Columbia. In: Current Research, Part E, Geological Survey of Canada, Paper 89-1, pp. 145-154.
- ArcWest Exploration Inc., 2019. ArcWest Exploration Inc. expands Yellow Bowl porphyry copper-gold target, Todd Creek project. <<https://arcwestexploration.com/2019/11/27/arcwest-exploration-inc-expands-yellow-bowl-porphyry-copper-gold-target-todd-creek-project/>>, last accessed December 2021.
- Allard, D.J., 1993. Geology and metallogeny of the Stewart mining

- camp, northwestern British Columbia. British Columbia Ministry of Energy, Mines and Petroleum Resources, British Columbia Geological Survey Bulletin 85, 105 p.
- Alldrick, D.J., Dawson, G.L., Boshier, J.A., and Webster, I.C.L., 1986. Geology of the Kitsault River area (NTS 103P). British Columbia Ministry of Energy, Mines and Petroleum Resources, British Columbia Geological Survey Open File 1986-02, 1:50,000 scale.
- Ascot Resources Ltd., 2020. Ascot announces its initial 2020 exploration program including high-grade silver mineralization at Silver Hill. <<https://ascotgold.com/news-releases/2020/ascot-announces-its-initial-2020-exploration-program-including-high-grade-silver-mineralization-at-silver-hill/>>, last accessed December 2021.
- Barresi, T., and Dostal, J., 2005. Geochemistry and petrography of upper Hazelton Group volcanics: VHMS-favourable stratigraphy in the Iskut River and Telegraph Creek map areas, northwestern British Columbia. In: Geological Fieldwork 2004, British Columbia Ministry of Energy and Mines, British Columbia Geological Survey Paper 2005-1, pp. 39-47.
- Barresi, T., Nelson, J.L., and Dostal, J., 2015. Geochemical constraints on magmatic and metallogenic processes: Iskut River Formation, volcanogenic massive sulfide-hosting basalts, NW British Columbia, Canada. *Canadian Journal of Earth Sciences*, 52, 1-20.
- Barrett, T.J., and Sherlock, R.L., 1996. Geology, lithochemistry and volcanic setting of the Eskay Creek Au-Ag-Cu-Zn deposit, northwestern British Columbia. *Exploration and Mining Geology*, 5, 339-368.
- Barrie, C.T., and Hannington, M.D., 1999. Classification of volcanic-associated massive sulfide deposits based on host-rock composition. In: Barrie, C.T., and Hannington, M.D., (Eds.), *Volcanic-associated massive sulfide deposits: processes and examples in modern and ancient settings*, Reviews in Economic Geology, 8, Society of Economic Geologists, Inc, pp. 1-11.
- Black, J.M., 1951. Geology and mineral occurrences of the Upper Kitsault Valley. In: British Columbia Ministry of Energy Mines and Petroleum Resources, British Columbia Geological Survey Annual Report, pp. A76-A83.
- Black, L.P., Kamo, S.L., Allen, C.M., Davis, D.W., Aleinikoff, J.N., Valley, J.W., Mundil, R., Campbell, I.H., Korsch, R.J., Williams, I.S., and Foudoulis, C., 2004. Improved $^{206}\text{Pb}/^{238}\text{U}$ microprobe geochronology by the monitoring of a trace-element-related matrix effect; SHRIMP, ID-TIMS, ELA-ICP-MS and oxygen isotope documentation for a series of zircon standards. *Chemical Geology* 205, 115-140.
- Brown, D.A., Gunning, M.H., and Greig, C.J., 1996. The Stikine project: Geology of western Telegraph Creek map area, northwestern British Columbia. British Columbia Ministry of Employment and Investment, British Columbia Geological Survey Bulletin 95, 130 p.
- Brueckner, S.M., Johnson, G., Wafforn, S., Gibson, H., Sherlock, R., Anstey, C., and McNaughton, K., 2021. Potential for volcanogenic massive sulfide mineralization at the A6 anomaly, northwest British Columbia, Canada: Stratigraphy, lithochemistry, and alteration mineralogy and chemistry. *Minerals*, 11, 867.
- Campbell, F.A., 1959. The geology of Torbrit Silver Mine, British Columbia. *Economic Geology*, 54, 1461-1495.
- Carter, N.C., 1981. Porphyry copper and molybdenum deposits, west-central British Columbia. British Columbia Ministry of Energy Mines and Petroleum Resources, British Columbia Geological Survey Bulletin 64, 81 p.
- Childe, F.C., 1997. Timing and tectonic setting of volcanogenic massive sulphide deposits in British Columbia: constraints from U-Pb geochronology, radiogenic isotopes, and geochemistry. Unpublished Ph.D. thesis, The University of British Columbia, Vancouver, B.C., Canada.
- Dawson, G.L., and Alldrick, D.J., 1986. Geology and mineral deposits of the Kitsault Valley. In: Geological Fieldwork 1985, British Columbia Ministry of Energy, Mines and Petroleum Resources, British Columbia Geological Survey Paper 1986-1, pp. 219-224.
- Devlin, B.D., 1987. Geology and genesis of the Dolly Varden silver camp, Alice Arm area, northwestern British Columbia. Unpublished M.Sc. thesis, The University of British Columbia, Vancouver, B.C., Canada.
- Devlin, B.D., and Godwin, C.I., 1986. Geology of the Dolly Varden camp, Alice Arm area. In: Geological Fieldwork 1985, British Columbia Ministry of Energy, Mines and Petroleum Resources, British Columbia Geological Survey Paper 1986-1, pp. 327-330.
- Dunne, K.P.E., and Pinsent, R.H., 2002. Depositional setting of silver-rich quartz-sulphate-carbonate deposits of the upper Kitsault River area, northwest British Columbia. In: Geological Fieldwork 2001, British Columbia Ministry of Energy, Mines and Petroleum Resources, British Columbia Geological Survey Paper 2002-01, pp. 177-196.
- Eggins, S.M., Kinsley, L., and Shelley, J., 1998. Deposition and element fractionation processes during atmospheric pressure laser sampling for analysis by ICP-MS. *Applied Surface Science* 127-129, 278-286.
- Eisbacher, G.H., 1981. Late Mesozoic-Paleogene Bowser Basin molasse and Cordilleran tectonics, western Canada. In: Miall, A. D. (Ed.), *Sedimentation and Tectonics in Alluvial Basins*, Geological Association of Canada Special Paper 23, pp. 125-151.
- Evenchick, C.A., and McNicoll, V.J., 2002. Stratigraphy, structure, and geochronology of the Anyox Pendant, northwest British Columbia, and implications for mineral exploration. *Canadian Journal of Earth Sciences*, 39, 1313-1332.
- Evenchick, C.A., and Thorkelson, D.J., 2005. Geology of the Spatsizi River map area, north-central British Columbia. *Geological Survey of Canada Bulletin* 577, 276 p.
- Evenchick, C.A., McMechan, M.E., McNicoll, V.J., and Carr, S.D., 2007. A synthesis of the Jurassic-Cretaceous tectonic evolution of the central and southeastern Canadian Cordillera: Exploring links across the orogen. In: Sears, J.W., Harms, T.A. and Evenchick, C.A., (Eds.), *Whence the mountains? Inquiries in the evolution of orogenic systems: A volume in honor of Raymond A. Price*, Geological Society of America Special Paper 433, pp. 117-145.
- Evenchick, C.A., Mustard, P.S., Greig, C.J., McMechan, M.E., Ritcey, D.H., Smith, G.T., and Ferri, F., 2008. Geology, Nass River, British Columbia. Geological Survey of Canada, Open File 5705, 1:125,000 scale.
- Evenchick, C.A., Poulton, T.P., and McNicoll, V.J., 2010. Nature and significance of the diachronous contact between the Hazelton and Bowser Lake groups (Jurassic), north-central British Columbia. *Bulletin of Canadian Petroleum Geology*, 58, 235-267.
- Febbo, G.E., Kennedy, L.A., Savell, M., Creaser, R.A., and Friedman, R.M., 2015. Geology of the Mitchell Au-Cu-Ag-Mo porphyry deposits, northwestern British Columbia, Canada. In: Geological Fieldwork 2014, British Columbia Ministry of Energy, Mines and Petroleum Resources, British Columbia Geological Survey Paper 2015-1, pp. 59-86.
- Febbo, G.E., Kennedy, L.A., Nelson, J.L., Savell, M.J., Campbell, M.E., Creaser, R.A., Friedman, R.M., van Straaten, B.I., and Stein, H.J., 2019. The evolution and structural modifications of the supergiant Mitchell Au-Cu porphyry, northwestern British Columbia. *Economic Geology*, 114, 303-324.
- Franklin, J.M., Gibson, H.L., Jonasson, I.R., and Galley, A.G., 2005. Volcanogenic massive sulfide deposits. In: Hedenquist, J.W., Thompson, J.F.H., Goldfarb, R.J., and Richards, J.P., (Eds.), *Economic Geology 100th Anniversary Volume*, The Economic Geology Publishing Company, pp. 523-560.
- Gagnon, J.-F., Barresi, T., Waldron, J.W.F., Nelson, J.L., Poulton, T.P., and Cordey, F., 2012. Stratigraphy of the upper Hazelton

- Group and the Jurassic evolution of the Stikine terrane, British Columbia. *Canadian Journal of Earth Sciences*, 49, 1027-1052.
- Galley, A.G., Hannington, M.D., and Jonasson, M., 2007. Volcanogenic massive sulphide deposits. In: Goodfellow, W.D., (Ed.), *Mineral deposits of Canada: A synthesis of major deposit types, district metallogeny, the evolution of geological provinces, and exploration methods*, Geological Association of Canada, Mineral Deposits Division, Special Publication 5, pp. 141-161.
- Gerstenberger, H., and Haase, G., 1997. A Highly effective emitter substance for mass spectrometric Pb isotopic ratio determinations. *Chemical Geology* 136, 309-312.
- Greig, C.J., 1991. Stratigraphic and structural relations along the west-central margin of the Bowser Basin, Oweegee and Kinskuch areas, northwestern British Columbia. In: *Current Research, Part A*, Geological Survey of Canada Paper 91-1A, pp. 197-205.
- Greig, C.J., 1992. Jurassic and Cretaceous plutonic and structural styles of the Eagle Plutonic Complex, southwestern British Columbia, and their regional significance. *Canadian Journal of Earth Sciences*, 29, 793-811.
- Greig, C.J., and Gehrels, G.E., 1995. U-Pb zircon geochronology of Lower Jurassic and Paleozoic Stikinian strata and Tertiary intrusions, northwestern British Columbia. *Canadian Journal of Earth Sciences*, 32, 1155-1171.
- Gibson, H.L., Morton, R.L., and Hudak, G.J., (1999). Submarine volcanic processes, deposits and environments favorable for the location of volcanic-associated massive sulfide deposits. In: Barrie, C.T., and Hannington, M.D., (Eds.), *Volcanic-associated massive sulfide deposits: processes and examples in modern and ancient settings*, Reviews in Economic Geology, 8, pp. 13-51.
- Grove, E.W., 1986. Geology and mineral deposits of the Stewart area, British Columbia. British Columbia Ministry of Energy, Mines and Petroleum Resources, British Columbia Geological Survey Bulletin 58, 219 p.
- Hannington, M.D., De Ronde, C.E.J., and Petersen, S., 2005. Sea-floor tectonics and submarine hydrothermal systems. In: Hedenquist, J.W., Thompson, J.F.H., Goldfarb, R.J., and Richards, J.P., (Eds.), *Economic Geology 100th Anniversary Volume*, The Economic Geology Publishing Company, pp. 111-141.
- Hanson, G., 1922. Upper Kitsault Valley, British Columbia. In: *Geological Survey of Canada, Summary Report Part A*, pp. 7-21.
- Herriott, T.M., Crowley, J.L., Schmitz, M.D., Wartes, M.A., and Gillis, R.J., 2019. Exploring the law of detrital zircon: LA-ICP-MS and CA-TIMS geochronology of Jurassic forearc strata, Cook Inlet, Alaska, USA. *Geology*, 47, 1044-1048.
- Höy, T., 1991. Volcanogenic massive sulphide deposits in British Columbia. In: McMillan, W.J., (Ed.), *Ore Deposits, Tectonics and Metallogeny in the Canadian Cordillera*, British Columbia Ministry of Energy, Mines and Petroleum Resources, British Columbia Geological Survey Paper 1991-4, pp. 89-124.
- Hunter, R.C., and van Straaten, B.I., 2020. Preliminary stratigraphy and geochronology of the Hazelton Group, Kitsault River area, Stikine terrane, northwest British Columbia. In: *Geological Fieldwork 2019*, British Columbia Ministry of Energy, Mines and Petroleum Resources, British Columbia Geological Survey Paper 2020-01, pp. 101-118.
- Hunter, R.C., Sebert, C.F.B., Friedman, R., and Wall, C., 2022. Geochronological data from the Kitsault River area: 2019 and 2020 field seasons. Ministry of Energy, Mines and Low Carbon Innovation, British Columbia Geological Survey, GeoFile.
- Jaffey, A.H., Flynn, K.F., Glendenin, L.E., Bentley, W.C., and Essling, A.M., 1971. Precision measurement of half-lives and specific activities of ^{235}U and ^{238}U . *Physical Review C*, 4, 1889-1906.
- Kyba, J., and Nelson, J.L., 2015. Stratigraphic and tectonic framework of the Kyber-Sericite-Pins mineralized trend, lower Iskut River, northwest British Columbia. In: *Geological Fieldwork 2014*, British Columbia Ministry of Energy, Mines and Petroleum Resources, British Columbia Geological Survey Paper 2015-01, pp. 41-58.
- Logan, J.M., and Mihalynuk, M.G., 2014. Tectonic controls on Early Mesozoic paired alkaline porphyry deposit belts (Cu-Au \pm Ag-Pt-Pd-Mo) within the Canadian Cordillera. *Economic Geology*, 109, 827-858.
- Logan, J.M., Drobe, J.R., and McClelland, W.C., 2000. Geology of the Forrest Kerr-Mess Creek area, northwestern British Columbia. British Columbia Ministry of Energy, Mines and Petroleum Resources, British Columbia Geological Survey Bulletin 104, 132 p.
- Ludwig, K.R., 2003. Isoplot 3.00, A Geochronological Toolkit for Microsoft Excel. University of California at Berkeley. kldwig@bgc.org/isoplot
- Ludwig, K.R., 2012. Isoplot 3.75. A geochronological toolkit for Microsoft Excel. Special Publication, Berkley Geochronology Center, 75 p.
- Marsden, H., and Thorkelson, D.J., 1992. Geology of the Hazelton volcanic belt in British Columbia: Implications for the Early to Middle Jurassic evolution of Stikinia. *Tectonics*, 11, 1266-1287.
- Marti, J., Gropelli, G., and Brum da Silveira, A., 2018. Volcanic stratigraphy: A review. *Journal of Volcanology and Geothermal Research* 357, 68-91.
- Mattinson, J.M., 2005. Zircon U-Pb chemical abrasion ("CA-TIMS") method: Combined annealing and multi-step partial dissolution analysis for improved precision and accuracy of zircon ages. *Chemical Geology* 220, pp. 47-66.
- McCuaig, M., and Sebert, C., 2017. 2016 Technical Report for the Dolly Varden Property, Skeena Mining Division. British Columbia Ministry of Energy, Mines and Petroleum Resources Assessment Report 36934.
- Macdonald, A.J., Lewis, P.D., Thompson, J.F.H., Nadaraju, G., Bartsch, R., Bridge, D.J., Rhys, D.A., Roth, T., Kaip, A., Godwin, C.I., and Sinclair, A.J., 1996a. Metallogeny of an Early to Middle Jurassic arc, Iskut River area, northwestern British Columbia. *Economic Geology*, 91, 1098-1114.
- MacDonald, R.W.J., Barrett, T.J., and Sherlock, R.L., 1996b. Geology and lithochemistry at the Hidden Creek massive sulfide deposit, Anyox, west-central British Columbia. *Exploration and Mining Geology*, 5, 369-398.
- MacIntyre, D., Ash, C., and Britton, J., 1994. Geological compilation Skeena-Nass area, west central British Columbia. In: British Columbia Ministry of Energy, Mines and Petroleum Resources, British Columbia Geological Survey Open File 1994-14, 1:250,000 scale.
- Miller, E.A., Kennedy, L.A., and van Straaten, B.I., 2020. Geology of the Kinskuch Lake area and Big Bulk porphyry prospect: Syn-depositional faulting and local basin formation during the Rhaetian (latest Triassic) transition from the Stuhini to the Hazelton Group. In: *Geological Fieldwork 2019*, British Columbia Ministry of Energy, Mines and Petroleum Resources, British Columbia Geological Survey Paper 2020-01, pp. 77-99.
- Monger, J.W.H., 1977. The Triassic Takla Group in McConnell Creek map-area, north central British Columbia. *Geological Survey of Canada Paper* 76-29, 45 p.
- Mortensen, J.K., and Kirkham, R.V., 1992. A U-Pb zircon age for host rocks of a syngenetic strontium(-zinc) occurrence in the Kitsault Lake area, west-central British Columbia. In: *Radiogenic Age and Isotopic Studies, Report 5*, Geological Survey of Canada, Paper 91.2, pp. 181-185.
- Mundil, R., Ludwig, K.R., Metcalfe, I., and Renne, P.R., 2004. Age and timing of the Permian Mass Extinctions: U/Pb Dating of Closed-System Zircons, *Science* 305, 1760-1763.
- Nelson, J.L., and Kyba, J., 2014. Structural and stratigraphic control of porphyry and related mineralization in the Treaty Glacier-KSM-Brucejack-Stewart trend of western Stikinia. In: *Geological Fieldwork 2013*, British Columbia Ministry of Energy, Mines and

- Petroleum Resources, British Columbia Geological Survey Paper 2014-01, pp. 111-140.
- Nelson, J.L., Colpron, M., and Israel, S., 2013. The Cordillera of British Columbia, Yukon and Alaska: Tectonics and metallogeny. In: Colpron, M., Bissig, T., Rusk, B.G., and Thompson, J., (Eds.), *Tectonics, Metallogeny and Discovery: The North American Cordillera and Similar Accretionary Settings*, Society of Economic Geologists Special Publication 17, pp. 53-110.
- Nelson, J.L., Waldron, J., van Straaten, B.I., Zagorevski, A., and Rees, C., 2018. Revised stratigraphy of the Hazelton Group in the Iskut River region, northwestern British Columbia. In: *Geological Fieldwork 2017*, British Columbia Ministry of Energy, Mines and Petroleum Resources, British Columbia Geological Survey Paper 2018-1, pp. 15-38.
- Paton, C., Hellstrom, J., Paul, B., Woodhead, J., and Hergt, J., 2011. Iolite: Freeware for the visualization and processing of mass spectrometric data. *Journal of Analytical Atomic Spectrometry* 26, 2508-2518.
- Peter, J.M., and Scott, S.D., 1999. Windy Craggy, northwestern British Columbia: The world's largest Besshi-type deposit. In: Barrie, C.T., and Hannington, M.D., (Eds.), *Volcanic-associated massive sulfide deposits: processes and examples in modern and ancient settings*, *Reviews in Economic Geology*, 8, Society of Economic Geologists, Inc., pp. 261-295.
- Pinsent, R.H., 2001. Mineral deposits of the upper Kitsault River area, British Columbia. In: *Geological Fieldwork 2000*, British Columbia Ministry of Energy and Mines, British Columbia Geological Survey Paper 2001-1, pp. 313-326.
- Pretium Resources Inc., 2021. Exploration - Near-mine and regional exploration. <<https://www.pretivm.com/exploration/Near-mine-and-Regional-Exploration/default.aspx>>, last accessed December 2021.
- Roth, T., Thompson, J.F.H., and Barrett, T.J., 1999. The precious metal-rich Eskay Creek deposit, northwestern British Columbia. In: Barrie, C.T., and Hannington, M.D., (Eds.), *Volcanic-associated massive sulfide deposits: processes and examples in modern and ancient setting*, *Reviews in Economic Geology* 8, pp. 357-374.
- Schmitz, M.D., and Schoene, B., 2007. Derivation of isotope ratios, errors, and error correlations for U-Pb geochronology using ^{205}Pb - ^{235}U -(^{233}U)-spiked isotope dilution thermal ionization mass spectrometric data. *Geochemistry, Geophysics, Geosystems*, 8, <<https://doi.org/10.1029/2006GC001492>>
- Scoates, J.S., and Friedman, R.M., 2008. Precise age of the platinumiferous Merensky Reef, Bushveld Complex, South Africa, by the U-Pb ID-TIMS chemical abrasion ID-TIMS technique, *Economic Geology*, 103, 465-471.
- Sherlock, R.L., Roth, T., Spooner, E.T.C., and Bray, C.J., 1999. Origin of the Eskay Creek precious metal-rich volcanogenic massive sulfide deposit; fluid inclusion and stable isotope evidence. *Economic Geology*, 94, 803-824.
- Sláma, J., Košler, J., Condon, D., and Crowley, J., 2008. Plešovice zircon-A new natural reference material for U-Pb and Hf isotopic microanalysis. *Chemical Geology* 249, 1-35.
- Smith, A.D., 1993. Geochemistry and tectonic setting of volcanics from the Anyox mining camp, British Columbia. *Canadian Journal of Earth Sciences*, 30, 48-59.
- Thirlwall, M.F., 2000. Inter-laboratory and other errors in Pb isotope analyses investigated using a ^{207}Pb - ^{204}Pb double spike. *Chemical Geology* 163, 299-322.
- Tipper, H.W., and Richards, T.A., 1976. Jurassic stratigraphy and history of north-central British Columbia. *Geological Survey of Canada Bulletin* 270, 82 p.
- Tupper, D.W., and McCartney, I.D., 1990. Geological, geochemical and diamond drilling report on the Kits-Jade project, Kitsault Lake area, British Columbia. Ministry of Energy, Mines and Petroleum Resources, British Columbia Geological Survey Assessment Report 20167, 23 p.
- Wiedenbeck, M., Alle, P., Corfu, F., Griffin, W.L., Meier, M., Oberli, F., Quadt, A.V., Roddick, J.C., and Spiegel, W., 1995. Three natural zircon standards for U-Th-Pb, Lu-Hf, trace element and REE analyses. *Geostandards Newsletter* 19, 1-23.
- Wiedenbeck, M., Hanchar, J.M., Peck, W.H., Sylvester, P., Valley, J., Whitehouse, M., Kronz, A., Morishita, Y., Nasdala, L., Fiebig, F., Franchi, I., Girard, J.P., Greenwood, R.C., Hinton, R., Kita, N., Mason, P.R.D., Norman, M., Ogasawara, M., Piccoli, P.M., Rhede, D., Satoh, H., Schulz-Dobrick, B., Skår, Ø., Spicuzza, M.J., Terada, K., Tindle, K., Togashi, S., Vennemann, T., Xie, Q., and Zheng, Y.F., 2004. Further characterization of the 91500 zircon crystal. *Geostandards and Geoanalytical Research* 28, 9-39.